1   **Selenoprotein S maintains intestinal homeostasis in ulcerative colitis by**

2   **inhibiting necroptosis of colonic epithelial cells through modulation of**

3   **macrophage polarization**

4   Yujie Yao[a, b], Tong Xu[a], Xiaojing Li[c], Xu Shi[a], Hao Wu[a], Ziwei Zhang[a, d, *], Shiwen Xu[a, d, *]

5   *a. College of Veterinary Medicine, Northeast Agricultural University, Harbin, 150030, PR China*

6   *b. School of Tropical Agriculture and Forestry, Hainan University, Haikou, 570228, PR China*

7   *c. College of Animal Science and Technology, Northeast Agricultural University, Harbin, 150030,*

8   *PR China*

9   *d. Key Laboratory of the Provincial Education Department of Heilongjiang for Common Animal*

10   *Disease Prevention and Treatment, College of Veterinary Medicine, Northeast Agricultural*

11   *University, Harbin, 150030, PR China*

12   * Corresponding author

13   *College of Veterinary Medicine, Northeast Agricultural University, Harbin, 150030, PR China*

14   *E-mail address:* zhangziwei@neau.edu.cn (Z. Zhang), shiwenxu@neau.edu.cn (S. Xu).

15   Contributor information:

16   Yujie Yao, Email: yujieyao@hainanu.edu.cn

17   Tong Xu, Email: 13147661321@163.com

18   Xiaojing Li, Email: xiaojingli@neau.edu.cn

19   Xu Shi, Email: 694478106@qq.com

20   Hao Wu, Email: S200601044@neau.edu.cn

21   Ziwei Zhang, Email: zhangziwei@neau.edu.cn

22   Shiwen Xu, Email: shiwenxu@neau.edu.cn

Abstract

Rationale: Macrophage polarization plays an important role in the inflammatory regulation of ulcerative colitis (UC). In this context, necroptosis is a type of cell death that regulates intestinal inflammation, and selenoprotein S (SelS) is a selenoprotein expressed in intestinal epithelial cells and macrophages that prevents intestinal inflammation. However, the underlying mechanisms of SelS in both cell types in regulating UC inflammatory responses remain unclear. Therefore, the direct effect of SelS deficiency on necroptosis in colonic epithelial cells (CECs) was investigated. In addition, whether SelS knockdown exacerbated intestinal inflammation by modulating macrophage polarization to promote necroptosis in CECs was assessed.

Methods: The UC model of SelS knockdown mice was established with 3.5% sodium dextran sulfate, and clinical indicators and colon injury were evaluated in the mice. Moreover, SelS knockdown macrophages and CECs cultured alone/cocultured were treated with IL-1β. The M1/M2 polarization, NF-κB/NLRP3 signaling pathway, oxidative stress, necroptosis, inflammatory cytokine, and tight junction indicators were analyzed. In addition, co-immunoprecipitation, liquid chromatography–mass spectrometry, laser confocal analysis, and molecular docking were performed to identify the interacting proteins of SelS. The GEO database was used to assess the correlation of SelS and its target proteins with macrophage polarization. The intervention effect of four selenium supplements on UC was also explored.

Results: Ubiquitin A-52 residue ribosomal protein fusion product 1 (Uba52) was identified as a potential interacting protein of SelS and SelS, Uba52, and yes-associated protein (YAP) was associated with macrophage polarization in the colon tissue of patients with UC. SelS deficiency in CECs directly induced reactive oxygen species (ROS) production, necroptosis, cytokine release,

45 and tight junction disruption. SelS deficiency in macrophages inhibited YAP ubiquitination

46 degradation by targeting Uba52, promoted M1 polarization, and activated the NF-κB/NLRP3

47 signaling pathway, thereby exacerbating ROS-triggered cascade damage in CECs. Finally,

48 exogenous selenium supplementation could effectively alleviate colon injury in UC.

49 **Conclusion:** SelS is required for maintaining intestinal homeostasis and that its deletion enhances

50 necroptosis in CECs, which is further exacerbated by promoting M1 macrophage polarization, and

51 triggers more severe barrier dysfunction and inflammatory responses in UC.

52

53 **Keywords:** Ulcerative Colitis, Macrophage Polarization, Selenoprotein S, Oxidative Stress,

54 Necroptosis

55

56 **Graphical Abstract:**
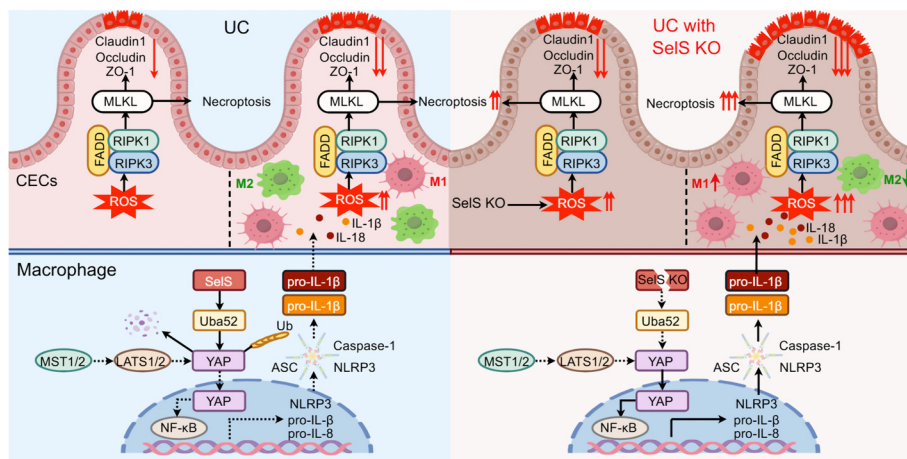
57

58 **Scheme**

59 Schematic diagram of selenoprotein S deficiency promoting M1 polarization aggravating

60 necroptosis of colonic epithelial cells in ulcerative colitis.

Introduction

Inflammatory bowel disease (IBD) is a chronic and relapsing inflammatory disease of the gastrointestinal tract, with Crohn's disease (CD) and ulcerative colitis (UC) as the primary disease patterns. Accumulated data from experimental models and clinical studies have indicated excessive immune cell infiltration and complex inflammatory networks as the main features of IBD [1]. Macrophages are the gatekeepers of intestinal immune homeostasis, and studies have shown that macrophage polarization may initiate and resolve intestinal inflammation in patients with IBD and animal colitis models [2]. In particular, M1 macrophages enhance tissue inflammation and exacerbate IBD damage, whereas M2 macrophages promote tissue repair and resolve inflammation to alleviate IBD symptoms [3]. Recent studies have shown that the expression of yes-related protein (YAP), a downstream regulator of the Hippo signaling pathway, is altered during local intestinal inflammation, affecting the conversion of M1 and M2 macrophages. Indeed, YAP inhibits M2 polarization and aggravates intestinal inflammation. Meanwhile, conditional YAP knockout (KO) in macrophages has been shown to prevent M1 polarization and alleviate colitis in mice [4]. However, the mechanism underlying the regulation of the M1/M2 switch and development of IBD remains unclear.

Intestinal epithelial cells (IECs) are essential for maintaining tissue homeostasis. However, excessive IECs death disrupts intestinal barrier integrity and leads to an inflammatory response in the lamina propria [5]. Necroptosis, a novel form of cell death modality that regulates intestinal homeostasis and inflammation, involves the activation of the protein kinases RIPK1 and RIPK3, followed by the phosphorylation of the executioner molecule MLKL to induce cellular membrane rupture and release damage-associated molecular patterns, interleukin-1β (IL-1β) and other

83   cytokines [6]. Reactive oxygen species (ROS) have been suggested to contribute to necroptosis,

84   although their origin and function in this process are not fully understood [7]. The important role of

85   necroptosis in certain inflammatory pathologies, such as IBD, sepsis, and neurodegenerative

86   diseases, has been widely reported [8]. Therefore, necroptosis inhibition is a potential therapeutic

87   strategy for many diseases involving inflammation and cell death. However, the role of IEC

88   necroptosis in the pathogenesis of IBD remains elusive.

89   Selenium is an essential trace mineral that participates in biological functions in the form of

90   selenoproteins with selenocysteine (Sec), as the active center. Epidemiological investigations and

91   clinical studies have identified reduced blood selenium level in patients with CD and UC [9, 10].

92   Indeed, selenium deficiency promoted inflammatory responses and exacerbated intestinal damage

93   in a mouse colitis model [11]. Of note, the switch from the M1 to M2 phenotype of macrophages in

94   the resolution phase of inflammation perhaps depends on the sufficient availability of selenium [12].

95   Selenium supplementation to sodium dextran sulfate (DSS)-treated mice suppressed M1 markers

96   and upregulated M2 markers in the colon tissue [13]. However, the specific selenoproteins that

97   affect macrophage polarization in UC remain unclear. The antioxidant and anti-inflammatory

98   functions of selenoproteins suggest that they act as mediators to exert the beneficial effects of

99   selenium in the gut, particularly via key roles played by them in host immune cells [14]. A study on

100   macrophage-specific Sec-tRNASec conditional KO mice revealed that selenoproteins in

101   macrophages were critical for protecting against severe gastrointestinal injury and promoting

102   efficient resolution [15]. In addition, selenoprotein W (SelW) suppressed Th1 cell differentiation by

103   promoting ROS scavenging in CD [16]. Speckmann et al. indicated that selenoprotein S (SelS) was

104   elevated in inflamed versus noninflamed ileal tissue of patients with CD [17]. Furthermore, studies

on the RAW264.7 cell line have shown that SelS regulated the release of cytokines from macrophages [18], indicating that SelS may be involved in regulating intestinal immune responses. Although high SelS levels have been found in IECs and intestinal macrophages [17], little is currently known about its exact function in the intestine, particularly regarding the mechanism of SelS in regulating UC colonic epithelial damage caused by macrophage polarization. The present study revealed that SelS expression was increased specifically and severely in the colon of UC mice, whereas SelS KO promoted M1 polarization and exacerbated colonic epithelial cell (CEC) injury. Mechanistically, SelS deficiency in CECs induced ROS overproduction, necroptosis, inflammatory factor release, and tight junction dysfunction, and SelS deficiency in macrophages reduced the expression of the target protein ubiquitin A-52 residue ribosomal protein fusion product 1 (Uba52) to inhibit the ubiquitination degradation of YAP and promote the polarization of M1, which further exacerbated ROS burst-triggered injury in CECs. Of note, selenium supplementation promoted the expression of SelS and inhibited the severity and clinical symptoms of colitis in UC mice. These findings may enrich the biological functions of SelS and provide evidence that SelS regulates macrophage polarization to affect CEC injury, thereby simultaneously providing a theoretical basis for UC treatment and acting as a reference for comparative medicine.

Materials

Animals

All animal procedures were conducted in strict accordance with protocols approved by the Institutional Animal Care and Use Committee of Northeast Agricultural University (SRM-11). Wild-type (WT) C57BL/6J mice and SelS KO mice on C57BL/6J background were purchased from Cyagen Bioscienc Inc. (Jiangsu, China) and were bred under specific pathogen-free conditions with

127   a 12-h light/12-h dark cycle, an ambient temperature of 22 ± 2 °C and humidity of 30-70%. Mice

128   were co-housed with 4 mice per cage. The mice used at the beginning of the experiments were 8

129   weeks and weighed 25 ± 2 g. No gender bias was observed in both males and females.

UC mouse model and selenium supplementation intervention

131   WT mice and SelS KO mice were administered 3.5% DSS (Macklin, Shanghai, China) in drinking

132   water for 7 days. In the intervention experiment of selenium supplementation, sodium selenite

133   (Na_2SeO_3), κ-selenocarrageenan (Se-Car), selenomethionine (SeMet), and nano-selenium (Nano-

134   Se) were administered to WT mice by gavage at a dosage of 2 mg/kg selenium for 28 consecutive

135   days, and then the mice drank distilled water containing 3.5% DSS for the last 7 days. The severity

136   of colitis was scored by monitoring clinical disease activity through daily observations of the

137   following parameters: weight loss (0 points = 1% weight loss, 1 points = 1-5% weight loss, 2 points

138   = 6-10% weight loss, 3 points= 11-15% weight loss, and score 4 = >16% weight loss); stool dilution

139   (0 points = normal and well-formed, 1 points = very soft and formed, 2 points = mild diarrhea, 3

140   points = moderate diarrhea, 4 points = severe diarrhea); and bleeding stool score (0 points = no

141   occult blood, 1 points = slight occult blood, 2 points = moderate occult blood, 3 points = severe

142   occult blood, 4 points = gross bloody stool). The Disease Activity Index (DAI) was the mean of the

143   combined scores for weight loss, fecal consistency, and fecal occult blood. Mice were executed at

144   the end of modeling; colon length was measured and tissues were stored at -80°C for backup.

Histology and histopathological score

146   The distal colon segments were fixed in 4% paraformaldehyde for 24 h, the tissues were sequentially

147   subjected to gradient ethanol dehydration, paraffin embedding, tissue sectioning, and hematoxylin

148   and eosin (H&E) staining. Images were recorded using an optical microscope (Thermo Fisher

149   Scientific, Waltham, MA, USA) to analyze morphology. The severity of colon injury was measured

150   based on the histopathological score of inflammatory cell infiltration, extent, hyperplasia, goblet

151   cell loss, ulceration, granulation tissue, and glandular rarefaction as previously described [19].

152   **Transmission electron microscopy (TEM) and ultrastructural score**

153   The distal colon segments were fixed with 2.5% glutaraldehyde, then treated with 1% Osmium

154   tetroxide, dehydrated with graded concentrations of ethanol, and embedded in a medium used for

155   electron microscopy. Ultrathin sections of the colon were cut onto formvar-coated slot grids, and

156   double-stained with 1% Uranyl acetate and 1% Lead citrate. Images were obtained with TEM

157   (Hitachi, Tokyo, Japan). For facilitate presentation, the degree of damage to microvilli, epithelial

158   cells, and tight junctions was scored according to the previous description [20].

159   **Cell culture and coculture**

160   Mouse macrophage (J774.1), mouse CEC (MCEC), and mouse hepatocarcinoma cell (Hepa1-6)

161   were cultured in complete Dulbecco's modified Eagle's medium (DMEM, Grand Island, New York,

162   USA) supplemented with 10% fetal bovine serum (FBS, HyClone, Logan, USA) and 1%

163   penicillin/streptomycin (Beyotime, Shanghai, China) at 37 °C in a humidified atmosphere with 5%

164   CO_2 strictly following aseptic protocol. The bone marrow-derived macrophages (BMDMs) were

165   obtained from WT and SelS KO mice according to the previously reported protocol [21]. In a

166   coculture assay of MCEC and J774.1, MCECs were seeded on the bottom of 24-well transwell

167   chamber plates, and J774.1 were seeded on top of 0.4-μm polycarbonate filter inserts in the transwell

168   chamber plates (Corning, New York, USA). For loss-of-function assay, J774.1 were transfected with

169   siNC (normal control) or siSelS. For inhibitor intervention assay, J774.1 were pretreated with YAP

170   inhibitor Verteporfin (VP, 0.32 μM) for 30 min. Subsequently, both cells were cocultured with

171 simultaneous exposure to 100 ng/mL IL-1β for 24 h. N-Acetylcysteine (NAC, 1 mM) was used to

172 scavenge intracellular ROS by treating MCECs 30 min before coculture.

siRNA transfection

174 J774.1 were transiently transfected with 50 nM of siRNA duplexes specific for SelS and Uba52

175 using Lipofectamine® RNAiMAX transfection reagent (Invitrogen, Carlsbad, CA, USA). BMDMs

176 and MCECs were also transfected with siRNA for SelS. Cell transfected with scrambled siRNA and

177 BLOCK-iT Alexa Fluor Red Fluorescent Oligo (Invitrogen, Carlsbad, CA, USA) were used as a

178 negative and positive control, respectively. Following small RNA sequences were used. SelS: 5′-

179 CAUGCAAGAAGGCAGAAGUUACAAA-3′,　Uba52:　5′-CCGACTACAACATCCAGAA-3′.

180 Cells were collected 48 hours after transfection for subsequent analysis.

Co-immunoprecipitation　(CoIP)

182 Whole-cell lysates were prepared by native lysis buffer with complete protease inhibitor cocktail

183 and phosphatase inhibitors. 1000 mg protein was incubated with 2 mg specific antibodies at 4 ℃

184 overnight with constant rotation, followed by incubation with 50% Protein A/G Agarose beads

185 (Absin Bioscience, Shanghai, China) for 2 h at 4 ℃. Subsequently, agarose beads were washed 3

186 times with lysis buffer and resuspended in an appropriate amount of SDS-PAGE loading buffer and

187 boiling for 10 min. Samples from immunoprecipitation or cell lysates were analyzed by

188 immunoblotting.

Liquid chromatograph-mass spectrometry (LC–MS) analysis

190 Hepa1-6 cells were transfected with empty plasmid and Flag-SelS overexpression plasmid,

191 respectively. After transfection for 48 h, cell lysates were purified with Anti-Flag M2 Affinity Gels

192 (Sigma Aldrich, Missouri, USA) and eluted with Flag peptides. The LC–MS analysis was carried

193   out by Sangon Biotech Co., Ltd. (Shanghai, China). Finally, we screened out the substrate proteins

194   that could bind to SelS according to the score and the mass of detected differentially expressed

195   proteins.

196   **Molecular docking**

197   Zdock software was applied to predict the binding direction and affinity between SelS and Uba52

198   proteins. The FASTA sequence of SelS was downloaded from the UniProt database and uploaded to

199   Swiss-Model for homology modeling. Simultaneously, the 3D structure for Uba52 (PDBID: 6JWI)

200   was chosen from the PDB database. Then the protein structure files of both were uploaded to Zdock

201   software for calculation, and the different docking solutions were ranked according to their energy

202   scores. Pymol 2.3.0 software was applied to observe the interaction pattern of the first-ranked

203   docking model.

204   **Detection of oxidative stress**

205   Commercial test kits purchased from Nanjing Jiancheng Bioengineering Institute were employed to

206   determine the contents of malonic dialdehyde (MDA) and glutathione (GSH), as well as the

207   activities of glutathione peroxidase (GPX), catalase (CAT), total superoxide dismutase (T-SOD),

208   and total antioxidant capacity (T-AOC). Specifically, fresh colon tissues were homogenized in cold

209   physiological saline solution. The supernatants obtained after centrifugation were used to measure

210   changes in these oxidative stress markers following the manufacturer's instructions. The 2′,7′-

211   dichlorodihydrofluorescein diacetate (DCFH-DA) probe provided by Nanjing Jiancheng

212   Bioengineering Institute was used to determine intracellular ROS accumulation in MCECs. After

213   the cells were incubated in serum-free medium containing 10 μM DCFH-DA for 30 min,

fluorescence images were obtained using a fluorescence microscope (Thermo Fisher Scientific, Waltham, MA, USA).

Cytokine assay

Colonic homogenates were prepared using saline, and the contents of TNF-α, IL-1β, IFN-γ, IL-6, IL-10, and IL-17 in the collected supernatants were assayed using ELISA kits (Jingmei Biotechnology, Jiangsu, China) according to the manufacturer's instructions.

Cell death assay

TdT-mediated dUTP nick-end labeling (TUNEL) staining was used to determine the apoptotic CECs in the colon tissue. 5 μm paraffin-embedded sections were incubated in a permeabilization solution and processed with the In Situ Apoptosis Detection Kit (Beyotime Biotechnology, Shanghai, China). In vitro, acridine orange/ethidium bromide (AO/EB) dual staining and flow cytometry were employed to analyze necroptotic MCECs. For AO/EB staining, cells were stained with a working solution containing 20 μL/mL AO and EB for 5 min, and the fluorescence signal was imaged under a fluorescence microscope. For flow cytometry, cells were labeled with Annexin V-FITC and propidine iodide (PI) according to the manufacturer's instructions (KeyGEN, Nanjing, China). Flowjo software provided a method for counting the rate of necroptosis.

Total RNA isolation and quantitative real-time PCR (qRT-PCR)

Total RNA was isolated from colon tissues and treated cells with TRIzol^{TM} reagent (Invitrogen, Carlsbad, CA, USA). An amount of 2 mg total RNA was reverse-transcribed to cDNA by using a cDNA first strand synthesis kit (Bioer, Hangzhou, China). qRT-PCR was performed on a LineGene 9600 Plus (Bioer, Hangzhou, China) with SYBR Green Master Mix (Bioer, Hangzhou, China). The

235   expression of individual genes was calculated with a 2-ΔΔCt method and normalized to the

236   expression of ACTB. Gene-specific primer sequences are shown in Table S1.

237   **Protein isolations and immunoblots**

238   Protein from colon tissues and treated cells were extracted using RIPA buffer containing protease

239   inhibitor (PMSF, Beyotime Biotechnology, Shanghai, China) and phosphatase inhibitor (PhosSTOP,

240   Roche). The protein concentration in the collected supernatants was determined by a BCA protein

241   assay kit (Solarbio, Beijing, China). For western blot (WB) analysis, equal amounts of protein

242   samples were separated by SDS-PAGE and transferred to nitrocellulose membranes (Pall

243   Corporation, New York, USA), which were incubated with the primary antibodies for SelS (Sigma,

244   HPA010025), Uba52 (Abcam, ab109227), YAP (ABclonal, A11264), p-YAP-S127 (ABclonal,

245   AP0489), MST1 (ABclonal, A12963), p-MST1/2-T180/T183 (ABclonal, AP1094), LATS1

246   (ABclonal, A17992), p-LATS1-S909/LATS2-S872 (ABclonal, AP0904), NF-κB (Wanleibio,

247   WL01980), p-NF-κB (Wanleibio, WL02169), NLRP3 (Wanleibio, WL02635), GSDMD-N

248   (ABclonal, A24059), ASC (Wanleibio, WL02462), Caspase-1 (Wanleibio, WL02996), IL-1β

249   (Wanleibio, WL00891), IL-18 (Wanleibio, WL01127), FADD (ABclonal, A19049), RIPK1

250   (ABclonal, A7414), p-RIPK1 (ABclonal, AP1230), RIPK3 (ABclonal, A5431), p-RIPK3 (ABclonal,

251   AP1408), MLKL (ABclonal, A19685), p-MLKL (ABclonal, AP1173), TNF-α (Wanleibio,

252   WL01581), IL-6 (Wanleibio, WL02841), IL-10 (Wanleibio, WL03088), Claudin1 (Wanleibio,

253   WL03073), Occludin (Wanleibio, WL01996), ZO-1 (Wanleibio, WL03419), Ub (ABclonal,

254   A18185), Flag (Sigma, F7425), HA (ABclonal, AE008), Myc (ABclonal, AE010), ACTB (ABclonal,

255   AC038), then incubated with HRP-conjugated secondary antibodies and visualized by using an ECL

kit (Biosharp, Hefei, China) in Azure Biosystem C300 imaging system (Thermo Fisher Scientific,

Waltham, MA, USA). ACTB was applied to verify equal protein loading.

Immunofluorescence

Colon sections and cells fixed with 4% PFA were permeabilized with 0.3% Triton X-100, then

blocked with blocking buffer for 2 h at room temperature and incubated overnight with specific

primary antibodies at 4 ℃. Subsequently, the samples were incubated with secondary antibody with

fluorescent label. Images were captured using a fluorescence microscope and quantitatively

analyzed with ImageJ.

GEO data analysis

The GSE75214 and GSE59071 datasets were obtained through the GEO Database

(https://www.ncbi.nlm.nih.gov/gds). Differential analysis was performed on the GSE75214 and

GSE59071 datasets separately using the R package limma (version 3.4.6) to obtain differential genes

between the comparison groups (UC and CD groups) and the control group. Next, Gene Set

Variation Analysis (GSVA package of R http://www.bioconductor.org/) was used to explore the

correlation between SelS, Uba52, YAP and the predefined, highly distinctive transcriptional profile

of each immune cell type. The classical chemokines and surface markers of both M1 and M2

macrophages were also included. Twenty-six types of immune cells with corresponding gene

signatures were utilized for analyses. Gene annotation and pathway enrichment analysis were

performed by the Database for Annotation, Visualization, and Integrated Discovery (DAVID), and

Kyoto Encyclopedia of Genes and Genomes (KEGG, http:// www.kegg.jp/kegg/pathway.html).

Quantification and statistical analysis

Statistical analysis was performed using GraphPad Prism 9 software. All data are given as the mean

± s.e.m of at least three biological replicates. Two groups were compared by unpaired *t*-test if data were normally distributed and otherwise by Mann-Whitney U test. Comparisons between multiple groups were done by one-way or two-way ANOVA with a Bonferroni multiple comparison post-test. Statistical significance was set at $p < 0.05$. In vitro significance was indicated as *$p < 0.05$, *$p < 0.01$, and ***$p < 0.001$. In vivo significance was indicated by different letters, with the same letter representing no difference significance and different letters representing difference significance.

Results

SelS ablation aggravates colon injury in UC mice

To investigate the role of SelS in colon injury in UC mice, the mRNA expression of 25 selenoproteins, including SelS, was assessed in the colon tissue of UC mice. Compared with the control group, SelS exhibited the highest expression abundance (81.94-fold) (Figure 1A). Its protein expression was significantly increased in the cytoplasm of macrophages (F4/80$^+$) and CECs (Villin$^+$) in the UC group (Figure 1B-C). To determine whether SelS plays a positive or negative role in UC, a genetic SelS KO mouse strain using CRISPR/CAS9-mediated genome engineering was established (Figure 1D-E). Under normal conditions, SelS KO mice displayed similar health status to WT mice. However, in the UC model mice, the feed intake, water intake, and body weight were significantly lower (Figure 1F-H); fecal consistency, fecal occult blood, and DAI scores were significantly increased (Figure 1I-L); and the colon segment from the cecum to rectum was shortened (Figure 1M). In addition, SelS KO mice exhibited more pronounced changes than WT mice. H&E staining revealed that inflammatory infiltration, infiltration extent, hyperplasia, goblet cell loss, ulceration, and glandular rarefaction in SelS KO mice with UC were more severe than those in WT mice with UC (Figure 1N-O). TEM showed that the damage to the microvillus,

epithelial cell, and tight junction in SelS KO mice was more pronounced than that in WT mice with

UC (Figure 1P-Q), indicating that SelS ablation exacerbates colonic histopathological and

microstructural damage in UC. The role of sex in colon injury was also assessed. Of note, males

exhibited more severe clinical symptoms and colonic lesions than females in both WT and SelS KO

mice. Considering that hormone secretion in females may interfere with inflammatory response and

thus inhibit UC development in clinical case analysis, male mice were selected for subsequent

experiments. Overall, these findings suggest that SelS exhibits a positive regulatory effect on colon

injury and that its inactivation worsens UC.

SelS ablation drives M1 polarization in UC colon by upregulating macrophage YAP expression

To elucidate the pathological significance of YAP in the SelS modulation of macrophage activity

and skewing in the UC colon, the infiltration and polarization of macrophages in the colon tissue

were determined. The results showed that SelS KO had no effect on the rising number of F4/80-

labeled macrophages in the UC colon (Figure S1) but that it promoted and inhibited the increase of

M1 and M2 macrophages, respectively (Figure 2A). Likewise, the mRNA expression of M1 and

M2 markers showed the same pattern in the colon of SelS KO mice with UC (Figure 2B). In addition,

SelS KO enhanced the activation of the NF-κB/NLRP3 pathway but did not alter GSDMD

expression (Figure 2C-E). Because IL-1β is an important inflammatory factor involved in the

inflammatory response during UC progression and significantly increased in the colon tissue of SelS

KO mice with UC (Figure 7A), the effect of SelS on macrophage polarization was analyzed by

treating SelS-knockdown macrophages with IL-1β in vitro. In agreement with the in vivo results,

the number of M1 macrophages and expression of associated genes at the mRNA level were

significantly augmented in SelS-deficient macrophages, and the opposite was observed in the M2

polarization assay (Figure 2F-G). Moreover, the silencing of SelS upregulated the expression of

genes related to the NF-κB/NLRP3 pathway without affecting GSDMD expression in J774.1

(Figure 2H-J), consistent with the results observed in colonic macrophages (Figure S7C) and

suggesting that SelS deletion has no effect on macrophage pyroptosis. Of note, exposing IL-1β-

treated siSelS J774.1 to the YAP inhibitor VP effectively reversed the polarization state of

macrophages (Figure 2K-L) and activation of the NF-κB/NLRP3 signaling pathway, again without

affecting GSDMD expression (Figure 2M-O). The same changes were observed in M1/M2

polarization, NF-κB/NLRP3 pathway, and GSDMD in BMDMs (Figure S2). Taken together, SelS

deficiency exacerbated M1 polarization in the UC colon by promoting YAP expression in

macrophages.

SelS-targeted Uba52 promotes ubiquitination degradation of macrophage YAP

protein in a proteasome-dependent manner instead of the Hippo pathway

To clarify the regulatory effect of SelS on YAP, Hippo signaling pathway-related indicators were

first examined. The results revealed that in vivo, the mRNA expression and phosphorylated protein

levels of MST1, LATS1, and YAP were unchanged in the colon tissue of UC and SelS KO mice

(Figure S3A-C). However, SelS KO significantly increased the total protein level of YAP (Figure

S3B-C), suggesting that the negative regulatory effect of SelS on YAP protein expression in the UC

colon is not regulated at the transcriptional level. In addition, the effect was not dependent on the

regulation of a series of kinase cascades upstream of the Hippo signaling pathway. Meanwhile, in

vitro, the treatment of J774.1 with IL-1β did not affect the mRNA expression and phosphorylated

protein levels of MST1, LATS1, and YAP (Figure S3D-I). However, the treatment increased the

344   total protein level of YAP in a time- and dose-dependent manner, except at 8 h (Figure S3E-F and

345   H-I), suggesting that IL-1β promoted macrophage YAP protein level at the post-translational stage,

346   independent of the traditional Hippo pathway.

347   To investigate how SelS regulates YAP expression in macrophages during UC development,

348   proteins interacting with SelS were determined using CoIP and LC–MS analysis in Hepa1-6 and the

349   obtained 372 differentially expressed proteins were analyzed using bioinformatics (Figure S4). CoIP

350   assay demonstrated that SelS physically associated with Uba52 in cotransfected J774.1 (Figure 3A).

351   In addition, immunofluorescence results indicated that SelS and Uba52 spatially colocalized in

352   J774.1 (Figure 3B). Besides, molecular docking analysis displayed the binding sites for SelS and

353   Uba52 (Figure 3C). These results confirmed the existence of interaction between Uba52 and SelS.

354   Meanwhile, compared with siNC J774.1, siUba52 J774.1 showed profoundly less ubiquitination of

355   YAP (Figure 3D), suggesting that Uba52 promotes the ubiquitination degradation of YAP. Next, the

356   protein stability of YAP was evaluated with the proteasome inhibitor MG132 and the protein

357   synthesis inhibitor cycloheximide (CHX). The results revealed that endogenous YAP protein

358   accumulated in the presence of MG132 from 2 h and further increased at 4 and 6 h after treatment

359   and that the protein expression of YAP in the siUba52 group was higher than that in the siNC group

360   at each time point (Figure 3E). The turnover rate of YAP protein detected with CHX in IL-1β-treated

361   J774.1 showed that the YAP protein level decreased gradually with the increase in time point and

362   the decline rate in the siUba52 group was lower than that of the siNC group (Figure 3F). These

363   results suggest that YAP is a short-lived protein in macrophages that is rapidly degraded via the

364   proteasomal pathway dependent on Uba52. SelS and Uba52 are known to interact while Uba52

365   negatively regulates YAP protein expression by promoting its ubiquitinated degradation. However,

366   the study results revealed YAP protein levels were always upregulated with the increasing mRNA

367   and protein levels of SelS and Uba52 in UC mice (Figure 3G-H and I-J) and IL-1β-treated J774.1

368   (Figure 3K-L and M-N), suggesting that other pathways regulate YAP expression. Furthermore, the

369   protein level of YAP in SelS KO mice and siSelS macrophages was upregulated with the decreasing

370   mRNA and protein levels of SelS and Uba52 (Figure 3G-N), providing strong evidence that SelS

371   negatively regulates YAP protein expression. Additional experiments revealed that IL-1β increased

372   the protein expression level of SelS, Uba52, and YAP in J774.1 in a dose-dependent manner (Figure

373   3O-P). However, with prolonged IL-1β stimulation, YAP protein levels reached a maximum at 6 h

374   but significantly decreased at the peak of SelS and Uba52 protein expression (8 h) (Figure 3Q-R),

375   indicating that SelS negatively regulates YAP stability in macrophages by targeting Uba52 to

376   promote its proteasome-dependent degradation.

377   **Correlation of SelS, Uba52, and YAP with immune cell types in individuals with**

378   **IBD revealed via GEO database mining**

379   A total of 194 and 116 sample data were obtained from the GSE75214 and GSE59071 datasets,

380   respectively. The GSE75214 dataset contains 22 healthy control, 97 UC, and 75 CD samples.

381   Differential expression analysis in this dataset yielded 979 DEGs, among which 518 were

382   upregulated and 416 downregulated. Meanwhile, the GSE59071 dataset includes data from 11

383   healthy control, 97 UC, and 8 CD samples, and differential expression analysis in this dataset

384   identified 911 DEGs, of which 598 were upregulated and 313 downregulated (Figure 4A). Next, the

385   differential expression of SelS, Uba52, and YAP in patients with IBD and healthy controls was

386   assessed. As shown in Figure 4B, the expression level of Uba52 and YAP in patients with UC was

387   significantly higher than that in healthy individuals in both the GSE75214 and GSE59071 datasets.

388   However, SelS was significantly increased only in the GSE75214 dataset. Meanwhile, no

389   differences in the expression level of the above three genes were observed between patients with

390   CD and healthy individuals in either dataset.

391   To investigate the possible impact of the three genes on the turbulence of the colonic immune

392   microenvironment during IBD onset, the correlation among SelS, Uba52, YAP, and 26 types of

393   immune cells, particularly macrophages, was explored using Pearson correlation analysis. In

394   patients with UC SelS was negatively correlated with M2 macrophages (cor = −0.338) and Uba52

395   was positively correlated with Th2 cells (cor = 0.509). Besides, YAP was positively associated with

396   10 immune cell types, including M1 (cor = 0.275) and M2 macrophages (cor = 0.333). In patients

397   with CD, SelS was negatively correlated with various immune cell types, including M2

398   macrophages (cor = −0.268), and Uba52 was positively correlated with both M2 (cor = 0.442) and

399   M1 macrophages (cor = 0.441). However, YAP was not correlated with the above 26 types of

400   immune cells (Figure 4C). Therefore, it was hypothesized that SelS, Uba52, and YAP exhibit

401   different response patterns to macrophage polarization in individuals with CD and UC. Next, the

402   association of SelS, Uba52, and YAP with the biomarkers of M1 and M2 macrophages in IBD

403   samples was analyzed. Significant correlation differences were observed in patients with UC and

404   CD, with SelS and YAP showing negative and positive correlation with the M1 markers, respectively,

405   in patients with UC (Figure 4D) and Uba52 exhibiting positive correlation with both M1 and M2

406   markers in patients with CD (Figure 4E). To assess the function of SelS, Uba52, and YAP in

407   modulating macrophage polarization, these three genes as well as M1 and M2 biomarkers were used

408   as gene ensembles to identify potential biological pathways. For this, Gene Ontology (GO) analysis

409   revealed multiple biological processes. These included the production of cytokines involved in

immune responses, production of the molecular mediators of immune responses, regulation of

inflammatory responses, positive regulation of immune effector processes, cellular responses to

oxidative stress, activation of macrophages, regulation of innate immune responses, and IκB

kinase/NF-κB signaling (Figure 4F). In addition, KEGG analysis revealed multiple pathways,

including cytokine–cytokine receptor interactions, inflammatory bowel disease, Toll-like receptor

signaling pathway, Th1 and Th2 cell differentiation, TNF-α signaling pathway, NOD-like receptor

signaling pathway, and chemokine signaling (Figure 4G).

Inhibition of YAP attenuates SelS ablation-induced M1 polarization, resulting in oxidative stress amelioration in CECs

Pathological damage in UC is generally accompanied by oxidative stress in the colonic epithelium.

Thus, whether SelS deficiency directly affects the redox status of CECs was investigated. Given

that macrophages create a specific microenvironment for oxidative damage in various cells by

employing a pro-inflammatory profile, whether SelS insufficiency changes the redox environment

in CECs by promoting M1 polarization was also assessed. As shown in Figure 5A, the MDA content

was increased, but the GSH content and GPX, CAT, T-SOD, and T-AOC activities in WT mice were

diminished in the UC model. SelS KO enhanced these changes compared with WT, indicating that

SelS deficiency aggravates oxidative stress in vivo. Meanwhile, higher ROS levels and lower SOD1,

SOD2, GST, and CAT mRNA expression were observed in IL-1β-treated MCECs of siSelS than

that with siNC treatment (Figure S5A-B), suggesting that SelS deletion in CECs directly induces

oxidative stress. In addition, ROS produced by MCECs alone or in combination with macrophages

(J774.1) exposed to IL-1β was significantly increase (Figure 5B-C), accompanied by reduced SOD1,

SOD2, GST, and CAT mRNA expressions in MCECs (Figure 5D). Moreover, ROS level was

432   abnormally increased and the aforementioned antioxidant gene expression was decreased in MCECs

433   cocultured with the J774.1 of siSelS compared with siNC. However, this phenomenon was reversed

434   by VP, which inhibited YAP expression in J774.1 (Figure S6A-C), suggesting that SelS deficiency

435   in macrophages promotes YAP-dependent M1 polarization and leads to oxidative stress in CECs.

436   Next, whether the redox imbalance of CECs is ameliorated by ROS-scavenging NAC was assessed.

437   As shown in Figure S6D-F, abnormal ROS level and antioxidant gene expression in MCECs

438   cocultured with J774.1 were restored to baseline under NAC treatment, indicating the beneficial

439   effect of NAC in attenuating oxidative stress.

440   **SelS ablation drives M1 polarization and exacerbates oxidative stress-mediated**

441   **necroptosis in CECs**

442   It is widely accepted that only the strict control of the proliferation and death of IECs can ensure the

443   integrity of the intestinal structure and maintenance of an effective intestinal barrier. Apoptosis,

444   pyroptosis, and necroptosis are programmed cell death forms closely related to UC. To unravel the

445   underlying mechanism through which SelS deficiency leads to worsening colon injury, Ki67,

446   TUNEL, and GSDMD immunofluorescence staining were performed using the colon tissue of WT

447   and SelS KO mice. The results revealed that despite the colon tissue of the UC group exhibiting

448   fewer Ki67-positive cells and more TUNEL- and GSDMD-positive cells compared with the Ctrl

449   group, no significant differences were observed between WT and SelS KO mice in the UC group

450   (Figure S7A-C), suggesting that SelS deletion does not aggravate colon injury by affecting

451   proliferation, apoptosis, and pyroptosis. Besides, immunofluorescence staining revealed an

452   increased expression of the necroptosis biomarkers RIPK1 and MLKL in the UC group compared

453   with the Ctrl group. Of note, the relative fluorescence intensity of RIPK1 and MLKL in the colon

21

454 tissue of SelS KO mice was dramatically higher than that in WT mice within the UC group (Figure

455 6A). Furthermore, the results of the quantitative analysis of necroptosis-related mRNA, total protein,

456 and phosphorylated protein were consistent (Figure 6B-D). Meanwhile, SelS knockdown

457 upregulated the necroptosis rate (Figure S8A-D) and the gene expression level of the necroptosis

458 markers (Figure. S8E-G) of MCECs treated with IL-1β. Therefore, these results indicate that the

459 occurrence of necroptosis is critical for SelS deficiency to aggravate colon injury. Additionally,

460 coculture with IL-1β-induced J774.1 upregulated the necroptosis rate (Figure 6E-F) and the gene

461 expression level of relevant necroptosis markers (Figure 6G-I) in MCECs. More importantly, a

462 necroptosis was substantially increased in MCECs cocultured with SelS-silenced J774.1 (Figure

463 S9A-D). However, these effects were corrected with the VP intervention of J774.1 (Figure S9A-D)

464 and NAC treatment of MCECs (Figure S9H-K), reversing the expression patterns of both mRNA

465 and proteins (Figure S9E-G and L-N). Thus, these results suggest that SelS deficiency induces M1

466 polarization by upregulating macrophage YAP expression, thereby promoting oxidative stress in

467 CECs and ultimately exacerbating necroptosis.

SelS ablation exacerbates inflammatory response depending on oxidative stress in

CECs induced by M1 polarization

470 Necroptosis is an inflammatory form of programmed cell death that plays a key role in driving

471 inflammation initiation and aggravation. As shown earlier, SelS deficiency exacerbates UC colon

472 injury primarily through CECs necroptosis. Therefore, the effect of SelS deletion on the

473 inflammatory response of colon tissue was next analyzed. As shown in Figure 7A, markedly

474 increased levels of several inflammatory factors, including TNF-α, IL-1β, IL-6, and IL-10 were

475 observed in the WT mice of the UC group compared with the Ctrl group. The increased level of pro-

476 inflammatory cytokines indicates the onset of an inflammatory response and the increase in IL-10

477 level may be compensatory to limit inflammatory exacerbation. Meanwhile, SelS KO mice

478 exhibited an elevated level of pro-inflammatory cytokines and an extremely reduced level of IL-10,

479 implying that the inflammatory response was amplified. However, IFN-γ and IL-17 levels were

480 significantly increased only in SelS KO mice with UC and the protein expression of inflammatory

481 factors showed the same trend as their mRNA expression (Figure 7B-C). In vitro, SelS knockdown

482 increased the gene expression of TNF-α, IL-1β, and IL-6 and decreased gene expression of IL-10

483 in MCECs treated with IL-1β (Figure S10A-C), suggesting that SelS deficiency in CECs directly

484 exacerbates intestinal inflammation in UC. The coculture of MCECs with IL-1β-induced J774.1 led

485 to the upregulated gene expression of TNF-α, IL-1β, and IL-6 and downregulated gene expression

486 of IL-10 in MCECs (Figure 7D-F). The SelS knockdown of J774.1 exacerbated the changing trend

487 of the abovementioned inflammatory factor gene expression in MCECs (Figure 7G-I), corroborating

488 that CECs necroptosis caused by SelS-silenced macrophages promotes inflammatory reaction.

489 However, these effects were effectively eliminated by the blockade of YAP expression in J774.1

490 (Figure 7G-I) and scavenging of ROS in MCECs (Figure 7J-L). In summary, these results suggest

491 that SelS deficiency induces M1 polarization by upregulating macrophage YAP expression, thereby

492 promoting ROS-mediated necroptosis in CECs and inducing a cytokine storm.

493 **SelS ablation aggravates tight junction dysfunction depending on oxidative stress**

494 **in CECs induced by M1 polarization**

495 Gut barrier integrity is maintained by tight junction proteins. Necroptosis usually severely

496 downregulates these proteins, leading to increased gut permeability to microbial ligands and noxious

497 metabolites and ultimately to persistent and unresolved inflammation. To uncover the potential

mechanisms of SelS in affecting tight junction proteins, the expression of tight junction-related genes in the colon tissue of WT mice and SelS KO mice was evaluated. As shown in Figure 8A-C, the mRNA and protein levels of Claudin1, Occludin, and ZO-1 in the UC group were significantly downregulated compared with the Ctrl group. Within the UC group, the above gene expression in SelS KO mice showed a greater downward trend than that in WT mice. Meanwhile, SelS knockdown downregulated the gene expression of Claudin1, Occludin, and ZO-1 in MCECs treated with IL-1β (Figure S10D–F). These results indicated that SelS deficiency in CECs directly exacerbates UC barrier damage. Meanwhile, the coculture of MCECs with J774.1 under IL-1β stimulation led to a reduction the above gene expression in MCECs (Figure 8D-F) and the expression of these tight junction genes in MCECs cocultured with siSelS J774.1 was lower than that in cells cocultured with siNC J774.1 (Figure 8G-I), indicating that macrophage SelS ablation triggers tight junction impairment in CECs. Next, to determine the role of macrophage polarization and oxidative stress in CECs in this process, J774.1 and MCECs were treated with VP and NAC, respectively. qRT-PCR revealed that the above interventions effectively inhibited the downregulation of tight junction-associated gene mRNA expression induced with SelS silencing (Figure 8G and J). In line with this, the expression pattern of the corresponding proteins was the same as that of the mRNA (Figure 8H-I and K-L). Taken together, these results suggest that the SelS ablation-induced impairment of tight junctions is mediated by exacerbating YAP-induced M1 polarization and ROS overproduction in CECs.

Selenium supplementation ameliorates colon injury in UC

As a critical trace element, selenium is considered as beneficial for the treatment of various intestinal diseases. To confirm whether selenium supplementation can attenuate colon injury in UC, UC mice

24

were administered selenium in the form of four selenium preparations, including Na_2SeO_3, Se-Car,

SeMet, and Nano-Se, via gavage. In general, selenium supplements increased feed intake, water

intake, and body weight in UC mice (Figure 9A-C). In particular, Nano-Se significantly decreased

fecal consistency, fecal occult blood, and DAI scores compared with UC mice (Figure 9D-G).

Likewise, colonic shortening (Figure 9H-I) as well as elevated microstructural (Figure 9J-K) and

ultrastructural (Figure 9L-M) damage scores in UC mice were effectively ameliorated with selenium

supplementation, with the most pronounced intervention effect observer with SeMet and Nano-Se.

These results indicated that exogenous selenium supplementation helps improve the clinical

manifestations of UC colon injury. Meanwhile, exogenous selenium supplementation is known to

promote the induction of multiple selenoproteins. Therefore, whether selenium supplementation

attenuates colon injury in UC by regulating SelS and its target proteins was next assessed. As shown

in Figure 9N-O, compared with the UC group, the four selenium preparations increased the protein

expression of SelS and Uba52 to varying degrees and decreased the protein expression of YAP,

implying that selenium supplementation promotes SelS expression to upregulate Uba52, and

subsequently suppresses of YAP expression.

The impact of selenium preparations on the macrophage polarization of the UC colon was next

investigated. qRT-PCR revealed that the expression of the M1 markers iNOS, TNF-α, IL-6, IL-12,

MCP-1, and MIG was significantly reduced after selenium supplementation in WT mice with UC

(Figure S11A). By contrast, the expression of the M2 markers, CCL24, MRC1, Arg1, IL-4, IL-10,

and Fizz1 was upregulated in selenium-supplemented mice (Figure S11B). These findings indicated

an inadequate and enhanced expression of M1 and M2 markers, respectively, in the UC colon after

selenium supplementation. The effect of selenium preparations on the redox state of the UC colon

542   was also evaluated. As expected, selenium treatment reduced the MDA level and increased the GSH

543   level and GPX, CAT, T-SOD, and T-AOC activities (Figure S11C). Additionally, the levels of

544   proteins associated with the NF-κB/NLRP3 signaling pathway (Figure S11D-E), necroptosis

545   (Figure S11F-G), and inflammatory cytokines (Figure S11H-I) was significantly reduced and the

546   level of tight junction proteins (Figure S11J-K) was significantly increased in selenium-

547   supplemented mice compared with UC mice. In the descender order, the ameliorative effect of

548   selenium preparations on colon injury in UC mice was Nano-Se > SeMet > Se-Car > Na_2SeO_3.

549   Taken together, these findings suggest that selenium supplementation ameliorates colon injury in

550   UC by suppressing M1 macrophages, oxidative stress, necroptosis, inflammatory factor release, and

551   tight junction damage. It appears that SelS targets Uba52 to regulate YAP in this process.

552   **Discussion**

553   Patients with IBD usually experience malabsorption and micronutrient deficiencies [22], and

554   selenium deficiency is a common manifestation in these patients [23, 24]. Because it exerts its

555   biological functions mainly through selenoproteins, the role of selenium and selenoproteins in UC

556   has received extensive attention [13]. In the present study, SelS deletion was shown to exacerbate

557   inflammatory response and intestinal epithelial damage in UC. In addition, SelS knockdown in

558   CECs led to ROS burst, necroptosis, inflammatory cytokine release, and tight junction disruption,

559   whereas SelS silencing in macrophages promoted M1 polarization, which exacerbated ROS-

560   dependent cascade damage in CECs and further worsened colon injury.

561   Growing evidence has suggested that some selenoproteins, such as thioredoxin reductase 3, SelP,

562   and SelW, regulate intestinal immune homeostasis [25-27]. SelS is a small type III single-pass

563   transmembrane selenoprotein with a Sec residue near the C-terminus at position 188 [28]. He et al.

564   demonstrated the protective anti-inflammatory effect of SelS using an siRNA knockdown strategy

565   in a lipopolysaccharide-induced sepsis mouse model [29]. In vitro, SelS gene expression was

566   increased due to pro-inflammatory cytokines [30], which may be a protective strategy, as SelS

567   knockdown increased the mRNA expression of pro-inflammatory cytokines in RAW264.7

568   macrophages [31]. The current study results revealed that SelS expression in the CECs and colonic

569   macrophages of UC mice showed an increasing trend. In addition, the DAI score, histopathological

570   damage score, and inflammatory cytokine level in SelS KO mice with UC were increased,

571   suggesting a protective role for SelS in intestinal inflammatory injury in UC. Pathological studies

572   have confirmed the presence of significant immune cell infiltration in the diseased mucosal tissue

573   of patients with UC, including macrophages [32]. Besides, changes in macrophage polarization and

574   related signaling pathways have been reported to have a vital impact on intestinal inflammation [33].

575   YAP, a critical regulator of macrophage polarization, drives macrophages toward M1 polarization

576   while restricting M2 polarization [34]. Zhou et al. reported that YAP could bind to IL-6 promoter

577   and enhance IL-6 production in bowel tissues [4]. Liu et al. demonstrated that YAP binds directly

578   to Arg1 promoter and inhibits Arg1 expression [34, 35]. More interestingly, YAP expression was

579   differentially regulated during the induction of macrophage polarization. Other studies

580   demonstrated that IL-4/IL-13 treatment inhibited YAP expression while LPS/IFN-γ stimulation

581   increased YAP protein expression in macrophages [36]. In the present study, SelS deletion

582   upregulated YAP expression, promoted M1 polarization, inhibited M2 polarization, and activated

583   the NF-κB/NLRP3 signaling pathway in colon tissues and macrophages without exacerbating

584   pyroptosis, in which the regulatory effects of other NLRP inflammasomes may be involved.

585   Moreover, the alteration in macrophages was reversed with the YAP inhibitor VP, indicating that

SelS affects macrophage polarization status via the negative regulation of YAP. The current dogma of YAP regulation is that the phosphorylation of YAP by upstream kinases in the Hippo signaling pathway is responsible for its ubiquitination and degradation [37]. Surprisingly, the current study results revealed a novel mechanism of YAP regulation in a Hippo-independent manner by promoting YAP ubiquitination through Uba52-targeting SelS, thereby expanding the scope of YAP regulation. Additionally, GEO data mining analysis revealed that the expression level of SelS, Uba52, and YAP was higher in the colon of patients with UC than in normal subjects, which was consistent with the changes in gene expression detected in the colon of UC mice. Of note, these three genes were closely associated with multiple immune cell infiltration in patients with UC, including M1 and M2, which provided further support for the study findings.

It is widely recognized that heightened ROS production-mediated redox imbalance is associated with intestine damage. Clinical studies have determined increased total oxidative stress index and decreased antioxidant capacity in the plasma of patients with UC. The inflamed colonic mucosa of patients with IBD and animals with experimental colitis produces more ROS and less GSH than the normal colonic mucosa [38, 39]. Ding et al. found that increased SelS expression inhibited intestinal oxidative stress in piglets [40]. In the present study, the increase in pro-oxidant indicators and decrease in antioxidant enzyme activities were more pronounced in SelS-deficient colon tissues and CECs, demonstrating that SelS deficiency promotes oxidative stress in the CECs of UC. Hu et al. mimicked the microenvironment of enteritis by LPS treatment of cocultured RAW264.7 macrophages and intestinal epithelial-like Caco-2 cells and found a significant increase in cellular ROS levels [41]. Moreover, ROS production was increased and antioxidant gene expression was downregulated in CECs cocultured with SelS-knockdown macrophages. Meanwhile. The VP and

NAC treatment of macrophages and CECs, respectively, was effective in ameliorating the redox status of CECs because the two cell types did not come into direct contact but interacted through paracrine cytokines. These findings suggest that SelS deletion promotes the polarization of M1 by upregulating YAP and stimulates the production of more pro-inflammatory cytokines that act on CECs, thereby increasing the level of oxidative stress in the latter.

Research has shown that diffuse inflammatory cell infiltration and small intestinal mucosal crypt abscesses in colitis promote excessive ROS production, leading to oxidative stress damage in colonocytes, increased epithelial barrier permeability, and pathogen invasion while exacerbating inflammatory cell infiltration and inflammatory injury [42]. Studies have shown that intracellular ROS accumulation in response to external inflammatory substances triggers necroptosis [7], which induces an inflammatory response in IECs and alters their cell membrane permeability [43]. Recent studies have shown that RIPK3 expression in the colon is positively correlated with the severity of UC [44]. Likewise, Pierdomenico et al. found that the expression level of RIPK3 and MLKL was significantly increased in the colon tissues of children with UC and CD and that the expression level of caspase-8 was markedly decreased, which is consistent with the fact that necroptosis occurs independent of caspase-8 but is dependent on RIPK3 and MLKL regulation [45]. Of note, the necroptosis inhibitor Nec-1 improved intestinal histopathology in DSS-induced colitis mice [44]. Other studies showed that SelS is unable to protect IEC from oxidative stress-induced apoptosis [17]. The present study indicated that SelS deficiency aggravated UC colon injury by inducing CEC necroptosis, independent of cell proliferation, apoptosis, and pyroptosis, thereby uncovering new evidence for the function of SelS in IECs. Li et al. studied the regulatory effect of SelS on necroptosis and demonstrated that SelS knockdown decreased mitochondrial membrane potential

630   and ATP depletion through increased ROS production, which, in turn, transformed apoptosis into

631   necroptosis [46]. Additionally, ROS produced by macrophages or other immune cells directly

632   damaged CECs during UC [47]. The present study results revealed that in a coculture system of

633   SelS-silenced macrophages and CECs, the inhibition of YAP expression in macrophages and ROS

634   production in CECs reduced the number of necrotic cells and expression of necroptosis-related

635   genes while decreasing the gene expression pro-inflammatory cytokines and increasing the gene

636   expression of anti-inflammatory cytokines and tight junctions. Therefore, SelS deficiency in

637   macrophage promotes YAP-mediated M1 polarization, thereby aggravating necroptosis,

638   inflammatory factor release, and tight junction impairment in CECs via ROS overproduction.

639   Serum selenium levels have been shown to be significantly lower in patients with quiescent UC

640   [48]. Data from animal studies suggest that adequate dietary selenium reduces intestinal

641   inflammation [49]. Indeed, the selenium status affects gene expression, signaling pathways, and

642   cellular functions in the gut. Related studies have proposed that several selenoproteins may be

643   involved in selenium-mediated protection against intestinal inflammation, including GPX isozymes,

644   SelS, and SelP, and that all of these selenoproteins may have immunomodulatory functions [12].

645   Barger et al. demonstrated that feeding selenium to mice in the form of Na_2SeO_3, selenium-enriched

646   yeast, and SeMet at a concentration of 1 mg/kg selenium induced a sustained upregulation of GPX1

647   and SelW [50]. The present study results showed that supplementation with different selenium

648   sources containing 2 mg/kg selenium effectively increased the protein level of SelS, accompanied

649   by an upregulation of Uba52 and downregulation of YAP. Other studies have confirmed that

650   selenium supplementation attenuated DSS-induced experimental colitis in WT mice. However,

651   selenium supplementation did not protect against DSS-induced colitis in mice that lacked

selenoprotein expression in macrophages [15], suggesting that selenoprotein expression in

macrophages is critical for the protective role of selenium in colitis. Besides, a study showed that

supplementation with a supra-nutritional dose of selenite (0.4 mg/mL) upregulated the expression

of M2 markers and concomitantly downregulated the expression of M1 markers in the colon tissue

of UC mice treated with the DSS [15]. The current study revealed similar effects on M1 and M2

markers in the colon tissue of UC mice supplementation with 2 mg/kg selenium. Moreover,

selenium supplementation reduced oxidative stress, inhibited necroptosis, decreased inflammatory

cytokine expression, and enhanced tight junction repair in the colon of UC mice. Of note, a previous

study revealed that GPX4 and SelS synergistically regulated oxidative stress-induced IEC damage

and that SelS exhibited a stronger regulatory effect [40]. Therefore, the regulatory effect of

exogenous selenium supplementation on UC may involve the interaction among multiple

selenoproteins, which deserves further exploration. Zhong et al. demonstrated that organic selenium

had a stronger modulatory effect on both inflammatory cytokines and tight junction proteins in the

colon tissue of UC mice than Na_2SeO_3 [51]. The present study demonstrated that the mitigating

effect of different forms of selenium on colon injury in UC mice varied greatly, with the extent of

effect being Nano-Se > SeMet > Se-Car > Na_2SeO_3, which may be attributed to their different

catabolic pathways and utilization of selenoprotein biosynthesis.

Conclusion

In summary, selenium is an essential micronutrient uniquely incorporated into various

selenoproteins to confer beneficial functions. In addition, SelS deficiency not only directly induces

oxidative stress, necroptosis, inflammatory factor release, and tight junction injury in CECs but also

enhances CEC injury by promoting YAP-mediated M1 polarization via Uba52 downregulation in

macrophages, which ultimately aggravates colon injury in UC. Meanwhile, selenium

supplementation, which upregulated SelS expression to some extent, may be a possible strategy to

alleviate macrophage polarization and mitigate CEC injury in UC. Of note, the effect of Nano-Se

was the strongest among the selenium supplements. Taken together, the study results elucidated the

mechanism through which SelS regulates the immunity of UC colonic mucosa and provided an

important therapeutic target to improve the inflammatory response and epithelial damage in UC

colon tissues.

Author contributions

Conceptualization, Y.Y., Z.Z., and S.X.; Methodology, Y.Y., Z.Z., and S.X.; Investigation, Y.Y., T.X.,

X.L., and X.S; Data Curation, Y.Y. and H.W.; Visualization, T.X., X.L., X.S. and H.W.; Writing –

Original Draft, Y.Y. and T.X.; Writing – Review & Editing, Z.Z. and S.X.; Supervision, S.X. All

authors read and approved the manuscript.

Data availability

All data generated or analyzed during this study are included in this article and its supplementary

data files and all original data are available from the corresponding authors upon request.

Competing interests

The authors declare no competing interests.

References

1.   Abraham C, Cho JH. Inflammatory bowel disease. N Engl J Med. 2009; 361: 2066-78.

2.   Na YR, Stakenborg M, Seok SH, Matteoli G. Macrophages in intestinal inflammation and resolution: a potential therapeutic target in IBD. Nat Rev Gastroenterol Hepatol. 2019; 16: 531-43.

3.   Du Y, Rong L, Cong Y, Shen L, Zhang N, Wang B. Macrophage polarization: an effective approach to targeted therapy of inflammatory bowel disease. Expert Opin Ther Targets. 2021; 25: 191-209.

4.   Zhou X, Li W, Wang S, Zhang P, Wang Q, Xiao J, et al. YAP Aggravates Inflammatory Bowel Disease by Regulating M1/M2 Macrophage Polarization and Gut Microbial Homeostasis. Cell Rep. 2019; 27: 1176-89 e5.

5.   Subramanian S, Geng H, Tan XD. Cell death of intestinal epithelial cells in intestinal diseases. Sheng Li Xue Bao. 2020; 72: 308-24.

6.   Pasparakis M, Vandenabeele P. Necroptosis and its role in inflammation. Nature. 2015; 517: 311-20.

7.   Fulda S. Regulation of necroptosis signaling and cell death by reactive oxygen species. Biol Chem. 2016; 397: 657-60.

8.   Choi ME, Price DR, Ryter SW, Choi AMK. Necroptosis: a crucial pathogenic mediator of human disease. JCI Insight. 2019; 4: e128834.

9.   Gentschew L, Bishop KS, Han DY, Morgan AR, Fraser AG, Lam WJ, et al. Selenium, selenoprotein genes and Crohn's disease in a case-control population from Auckland, New Zealand. Nutrients. 2012; 4: 1247-59.

10.   Ringstad J, Kildebo S, Thomassen Y. Serum selenium, copper, and zinc concentrations in Crohn's disease and ulcerative colitis. Scand J Gastroenterol. 1993; 28: 605-8.

11.   Barrett CW, Singh K, Motley AK, Lintel MK, Matafonova E, Bradley AM, et al. Dietary selenium deficiency exacerbates DSS-induced epithelial injury and AOM/DSS-induced tumorigenesis. PLoS One. 2013; 8: e67845.

12.   Speckmann B, Steinbrenner H. Selenium and selenoproteins in inflammatory bowel diseases and experimental colitis. Inflamm Bowel Dis. 2014; 20: 1110-9.

13.   Kudva AK, Shay AE, Prabhu KS. Selenium and inflammatory bowel disease. Am J Physiol Gastrointest Liver Physiol. 2015; 309: G71-7.

731 14. Ala M, Kheyri Z. The rationale for selenium supplementation in inflammatory bowel disease: A
732 mechanism-based point of view. Nutrition. 2021; 85: 111153.

733 15. Kaushal N, Kudva AK, Patterson AD, Chiaro C, Kennett MJ, Desai D, et al. Crucial role of
734 macrophage selenoproteins in experimental colitis. J Immunol. 2014; 193: 3683-92.

735 16. Huang LJ, Mao XT, Li YY, Liu DD, Fan KQ, Liu RB, et al. Multiomics analyses reveal a critical
736 role of selenium in controlling T cell differentiation in Crohn's disease. Immunity. 2021; 54: 1728-44 e7.

737 17. Speckmann B, Gerloff K, Simms L, Oancea I, Shi W, McGuckin MA, et al. Selenoprotein S is a
738 marker but not a regulator of endoplasmic reticulum stress in intestinal epithelial cells. Free Radic Biol
739 Med. 2014; 67: 265-77.

740 18. Curran JE, Jowett JB, Elliott KS, Gao Y, Gluschenko K, Wang J, et al. Genetic variation in
741 selenoprotein S influences inflammatory response. Nat Genet. 2005; 37: 1234-41.

742 19. Burrello C, Garavaglia F, Cribiu FM, Ercoli G, Lopez G, Troisi J, et al. Therapeutic faecal
743 microbiota transplantation controls intestinal inflammation through IL10 secretion by immune cells. Nat
744 Commun. 2018; 9: 5184.

745 20. Zhang L, Gui S, Liang Z, Liu A, Chen Z, Tang Y, et al. Musca domestica Cecropin (Mdc) Alleviates
746 Salmonella typhimurium-Induced Colonic Mucosal Barrier Impairment: Associating With Inflammatory
747 and Oxidative Stress Response, Tight Junction as Well as Intestinal Flora. Front Microbiol. 2019; 10:
748 522.

749 21. Toda G, Yamauchi T, Kadowaki T, Ueki K. Preparation and culture of bone marrow-derived
750 macrophages from mice for functional analysis. STAR protocols. 2021; 2: 100246.

751 22. Nielsen OH, Ainsworth M, Coskun M, Weiss G. Management of Iron-Deficiency Anemia in
752 Inflammatory Bowel Disease: A Systematic Review. Medicine (Baltimore). 2015; 94: e963.

753 23. Han YM, Yoon H, Lim S, Sung MK, Shin CM, Park YS, et al. Risk Factors for Vitamin D, Zinc,
754 and Selenium Deficiencies in Korean Patients with Inflammatory Bowel Disease. Gut Liver. 2017; 11:
755 363-9.

756 24. Weisshof R, Chermesh I. Micronutrient deficiencies in inflammatory bowel disease. Curr Opin Clin
757 Nutr Metab Care. 2015; 18: 576-81.

758 25. Short SP, Pilat JM, Williams CS. Roles for selenium and selenoprotein P in the development,
759 progression, and prevention of intestinal disease. Free Radic Biol Med. 2018; 127: 26-35.

760 26. Liu Q, Du P, Zhu Y, Zhang X, Cai J, Zhang Z. Thioredoxin reductase 3 suppression promotes colitis
761 and carcinogenesis via activating pyroptosis and necrosis. Cell Mol Life Sci. 2022; 79: 106.

762 27. Nettleford SK, Liao C, Short SP, Rossi RM, Singh V, Prabhu KS. Selenoprotein W Ameliorates
763 Experimental Colitis and Promotes Intestinal Epithelial Repair. Antioxidants (Basel). 2023; 12: 850.

764 28. Ghelichkhani F, Gonzalez FA, Kapitonova MA, Schaefer-Ramadan S, Liu J, Cheng R, et al.
765 Selenoprotein S: A versatile disordered protein. Arch Biochem Biophys. 2022; 731: 109427.

766 29. He L, Wang B, Yao Y, Su M, Ma H, Jia N. Protective effects of the SEPS1 gene on
767 lipopolysaccharide-induced sepsis. Mol Med Rep. 2014; 9: 1869-76.

768 30. Gao Y, Hannan NR, Wanyonyi S, Konstantopolous N, Pagnon J, Feng HC, et al. Activation of the
769 selenoprotein SEPS1 gene expression by pro-inflammatory cytokines in HepG2 cells. Cytokine. 2006;
770 33: 246-51.

771 31. Kim KH, Gao Y, Walder K, Collier GR, Skelton J, Kissebah AH. SEPS1 protects RAW264.7 cells
772 from pharmacological ER stress agent-induced apoptosis. Biochem Biophys Res Commun. 2007; 354:
773 127-32.

774 32. Kiremidjian-Schumacher L, Roy M, Wishe HI, Cohen MW, Stotzky G. Selenium and immune cell

775   functions. I. Effect on lymphocyte proliferation and production of interleukin 1 and interleukin 2. Proc

776   Soc Exp Biol Med. 1990; 193: 136-42.

777   33.   Maasfeh L, Hartlova A, Isaksson S, Sundin J, Mavroudis G, Savolainen O, et al. Impaired Luminal

778   Control of Intestinal Macrophage Maturation in Patients With Ulcerative Colitis During Remission. Cell

779   Mol Gastroenterol Hepatol. 2021; 12: 1415-32.

780   34.   Yimlamai D, Christodoulou C, Galli GG, Yanger K, Pepe-Mooney B, Gurung B, et al. Hippo

781   pathway activity influences liver cell fate. Cell. 2014; 157: 1324-38.

782   35.   Mia MM, Cibi DM, Abdul Ghani SAB, Song W, Tee N, Ghosh S, et al. YAP/TAZ deficiency

783   reprograms macrophage phenotype and improves infarct healing and cardiac function after myocardial

784   infarction. PLoS Biol. 2020; 18: e3000941.

785   36.   Luo Q, Luo J, Wang Y. YAP Deficiency Attenuates Pulmonary Injury Following Mechanical

786   Ventilation Through the Regulation of M1/M2 Macrophage Polarization. J Inflamm Res. 2020; 13: 1279-

787   90.

788   37.   Zhao B, Li L, Lei Q, Guan KL. The Hippo-YAP pathway in organ size control and tumorigenesis:

789   an updated version. Genes Dev. 2010; 24: 862-74.

790   38.   Zhang C, Wang H, Yang X, Fu Z, Ji X, Shi Y, et al. Oral zero-valent-molybdenum nanodots for

791   inflammatory bowel disease therapy. Sci Adv. 2022; 8: eabp9882.

792   39.   Buffinton GD, Doe WF. Depleted mucosal antioxidant defences in inflammatory bowel disease.

793   Free Radic Biol Med. 1995; 19: 911-8.

794   40.   Ding D, Mou D, Zhu H, Jiang X, Che L, Fang Z, et al. Maternal Organic Selenium Supplementation

795   Relieves Intestinal Endoplasmic Reticulum Stress in Piglets by Enhancing the Expression of Glutathione

796   Peroxidase 4 and Selenoprotein S. Frontiers in nutrition. 2022; 9: 900421.

797   41.   Hu X, Yu Q, Hou K, Ding X, Chen Y, Xie J, et al. Regulatory effects of Ganoderma atrum

798   polysaccharides on LPS-induced inflammatory macrophages model and intestinal-like Caco-

799   2/macrophages co-culture inflammation model. Food Chem Toxicol. 2020; 140: 111321.

800   42.   Reeves MA, Hoffmann PR. The human selenoproteome: recent insights into functions and

801   regulation. Cell Mol Life Sci. 2009; 66: 2457-78.

802   43.   Negroni A, Colantoni E, Pierdomenico M, Palone F, Costanzo M, Oliva S, et al. RIP3 AND pMLKL

803   promote necroptosis-induced inflammation and alter membrane permeability in intestinal epithelial cells.

804   Dig Liver Dis. 2017; 49: 1201-10.

805   44.   Duan C, Xu X, Lu X, Wang L, Lu Z. RIP3 knockdown inhibits necroptosis of human intestinal

806   epithelial cells via TLR4/MyD88/NF-kappaB signaling and ameliorates murine colitis. BMC

807   Gastroenterol. 2022; 22: 137.

808   45.   Pierdomenico M, Negroni A, Stronati L, Vitali R, Prete E, Bertin J, et al. Necroptosis is active in

809   children with inflammatory bowel disease and contributes to heighten intestinal inflammation. Am J

810   Gastroenterol. 2014; 109: 279-87.

811   46.   Li X, Chen M, Yang Z, Wang W, Lin H, Xu S. Selenoprotein S silencing triggers mouse hepatoma

812   cells apoptosis and necrosis involving in intracellular calcium imbalance and ROS-mPTP-ATP. Biochim

813   Biophys Acta Gen Subj. 2018; 1862: 2113-23.

814   47.   Pereira C, Gracio D, Teixeira JP, Magro F. Oxidative Stress and DNA Damage: Implications in

815   Inflammatory Bowel Disease. Inflamm Bowel Dis. 2015; 21: 2403-17.

816   48.   Geerling BJ, Badart-Smook A, Stockbrugger RW, Brummer RJ. Comprehensive nutritional status

817   in recently diagnosed patients with inflammatory bowel disease compared with population controls. Eur

818   J Clin Nutr. 2000; 54: 514-21.

819   49. Krehl S, Loewinger M, Florian S, Kipp AP, Banning A, Wessjohann LA, et al. Glutathione

820   peroxidase-2 and selenium decreased inflammation and tumors in a mouse model of inflammation-

821   associated carcinogenesis whereas sulforaphane effects differed with selenium supply. Carcinogenesis.

822   2012; 33: 620-8.

823   50. Barger JL, Kayo T, Pugh TD, Vann JA, Power R, Dawson K, et al. Gene expression profiling reveals

824   differential effects of sodium selenite, selenomethionine, and yeast-derived selenium in the mouse. Genes

825   Nutr. 2012; 7: 155-65.

826   51. Zhong Y, Jin Y, Zhang Q, Mao B, Tang X, Huang J, et al. Comparison of Selenium-Enriched

827   Lactobacillusparacasei, Selenium-Enriched Yeast, and Selenite for the Alleviation of DSS-Induced

828   Colitis in Mice. Nutrients. 2022; 14: 2433.

Figure legends
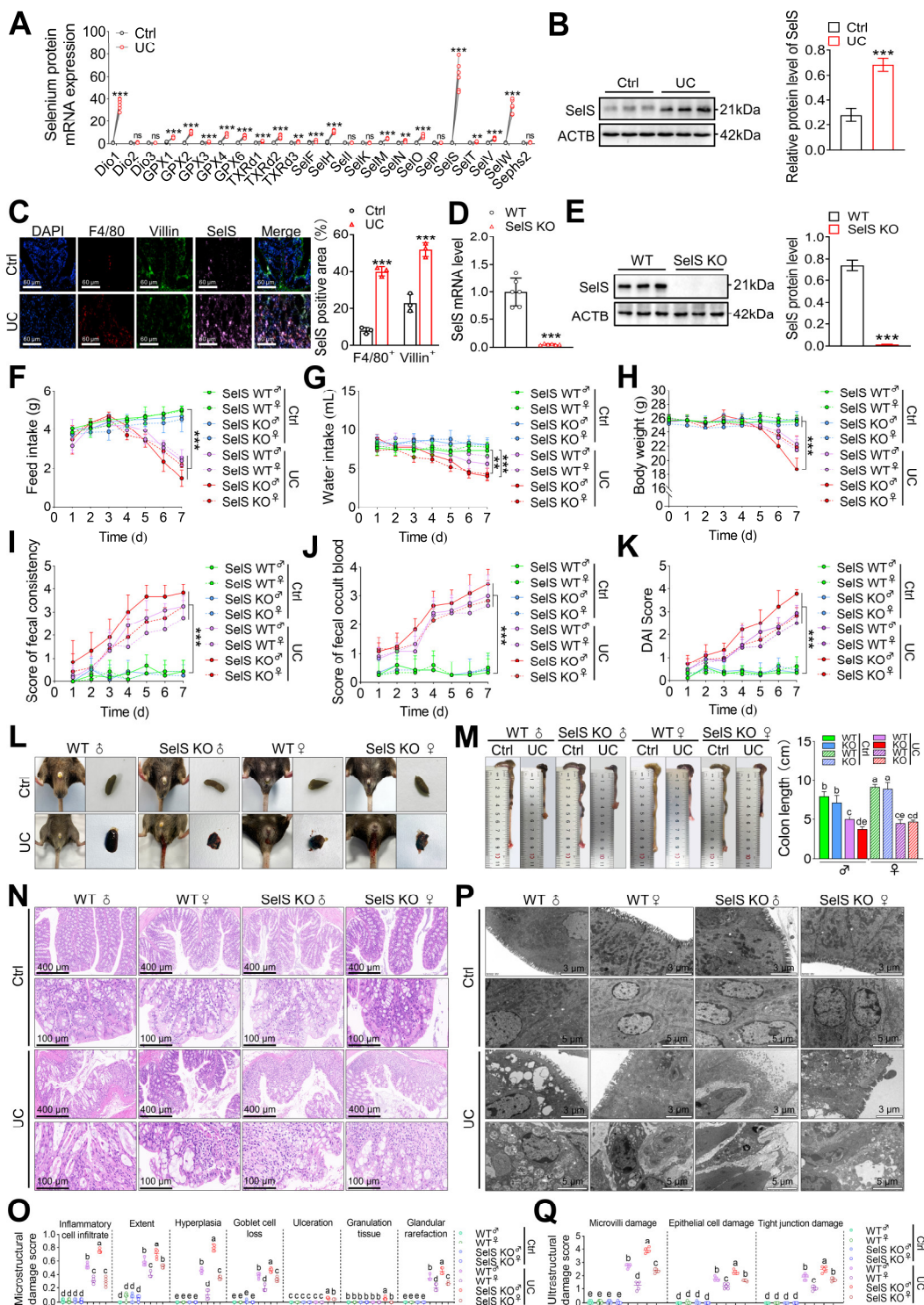
Figure 1. SelS deletion aggravates colon injury in UC mice. (A) Expression profile of 25
selenoproteins in the colon of WT mice with UC, n = 6. **(B)** SelS protein levels in the colon of WT
mice with UC, n = 3. **(C)** Immunofluorescence staining and quantitative analysis of F4/80, Villin,
and SelS in the colon of WT mice with UC, n = 3. Scale bar, 60 μm. **(D)** SelS mRNA expression in
the colon of WT mice and SelS KO mice, n = 6. **(E)** SelS protein level in the colon of WT mice and

836   SelS KO mice, n = 3. **(F-K)** Clinical indicators of WT and SelS KO mice in Ctrl and UC groups, n

837   = 6. **(F)** Feed intake. **(G)** Water intake. **(H)** Body weight. **(I)** Scores of fecal consistency. **(J)** Scores

838   of fecal occult blood. **(K)** DAI score. **(L)** Perianal area and feces appearance of WT and SelS KO

839   mice in Ctrl and UC groups. **(M)** Colon length of WT and SelS KO mice in Ctrl and UC groups, n

840   = 6. Different lowercase letters indicate significant differences between groups. **(N)** Representative

841   H&E slides of distal colon sections of WT and SelS KO mice in Ctrl and UC groups, n = 6. Scale

842   bar, 400 μm and 100 μm. **(O)** The microstructural damage score of the colon, n = 6. Different

843   lowercase letters indicate significant differences between groups. **(P)** Representative images of

844   TEM detection in Ctrl and UC groups for the colon of WT and SelS KO mice, n = 6. Scale bar, 3

845   μm and 5 μm. **(Q)** The ultrastructural damage score of the colon, n = 6. Different lowercase letters

846   indicate significant differences between groups.

847
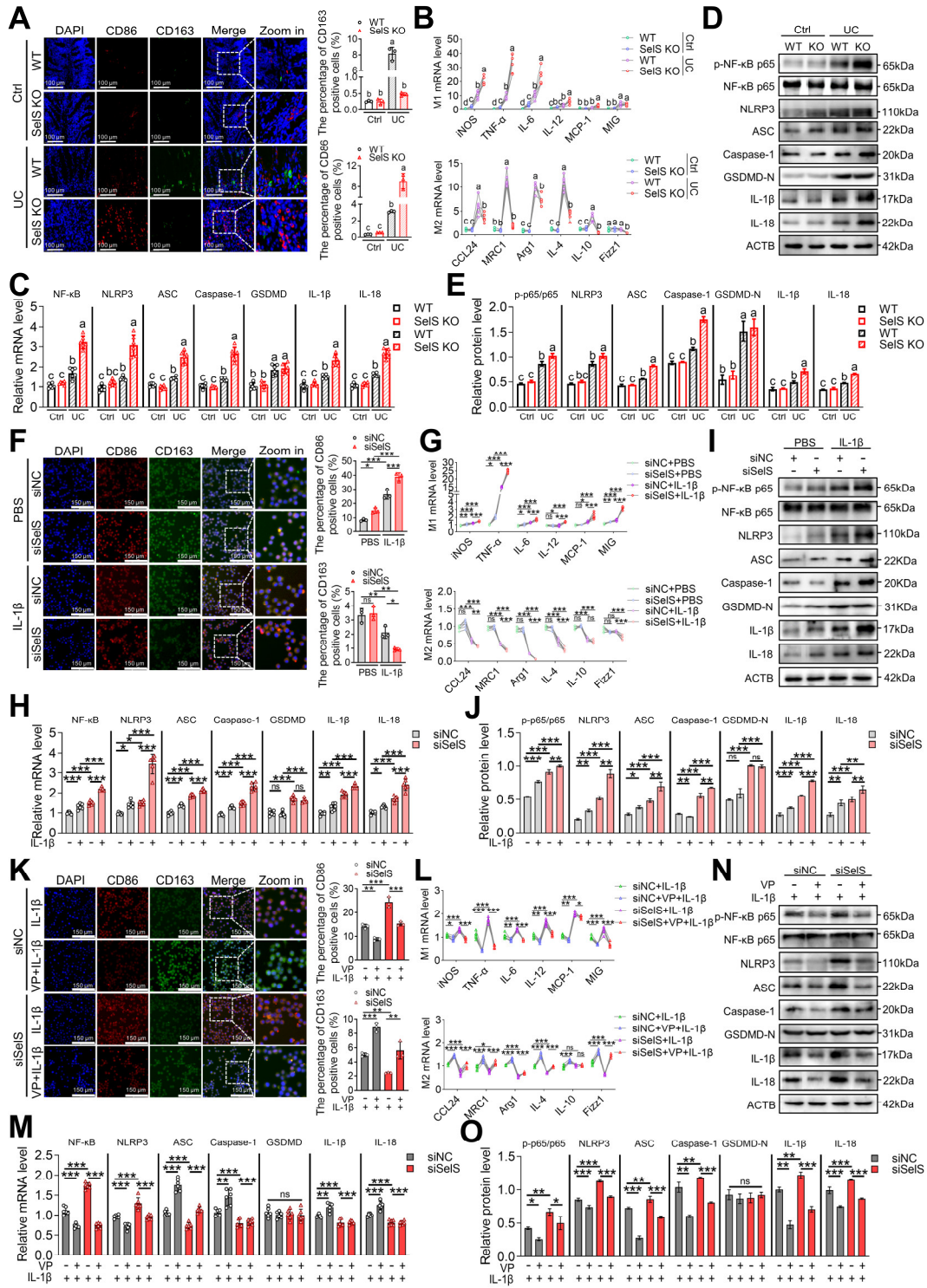
Figure 2. SelS ablation promotes YAP-mediated M1 polarization and NF-κB/NLRP3 pathway

activation. (A) Immunofluorescence staining and quantitative analysis of CD86 and CD163 in the

colon of WT and SelS KO mice in Ctrl and UC groups, n = 3. Scale bar, 100 μm. Different lowercase

letters indicate significant differences between groups. **(B)** mRNA expressions related to M1 and

852 M2 in the colon of WT and SelS KO mice in Ctrl and UC groups, n = 6. Different lowercase letters

853 indicate significant differences between groups. **(C)** mRNA expressions related to the NF-

854 κB/NLRP3 pathway and GSDMD in the colon of WT and SelS KO mice in Ctrl and UC groups, n

855 = 6. Different lowercase letters indicate significant differences between groups. **(D-E)** Protein levels

856 related to the NF-κB/NLRP3 pathway and GSDMD in the colon of WT and SelS KO mice in Ctrl

857 and UC groups, n = 3. Different lowercase letters indicate significant differences between groups.

858 **(F-J)** J774.1 transfected with siNC or siSelS were stimulated with PBS or IL-1β (100 ng/mL) for 6

859 h. **(F)** Immunofluorescence staining and quantitative analysis of CD86 and CD163 in J774.1, n = 3.

860 Scale bar, 150 μm. **(G)** mRNA expressions related to M1 and M2 in J774.1, n = 6. **(H)** mRNA

861 expressions related to the NF-κB/NLRP3 pathway and GSDMD in J774.1, n = 6. **(I-J)** Protein levels

862 related to the NF-κB/NLRP3 pathway and GSDMD in J774.1, n = 3. **(K-O)** J774.1 transfected with

863 siNC or siSelS were pretreated with or without VP (0.32 μM) for 30 min before PBS or IL-1β (100

864 ng/mL) stimulation for 6 h. **(K)** Immunofluorescence staining and quantitative analysis of CD86

865 and CD163 in J774.1, n = 3. Scale bar, 150 μm. **(L)** mRNA expressions related to M1 and M2 in

866 J774.1, n = 6. **(M)** mRNA expressions related to the NF-κB/NLRP3 pathway and GSDMD in J774.1,

867 n = 6. **(N-O)** Protein levels related to the NF-κB/NLRP3 pathway and GSDMD in J774.1, n = 3.
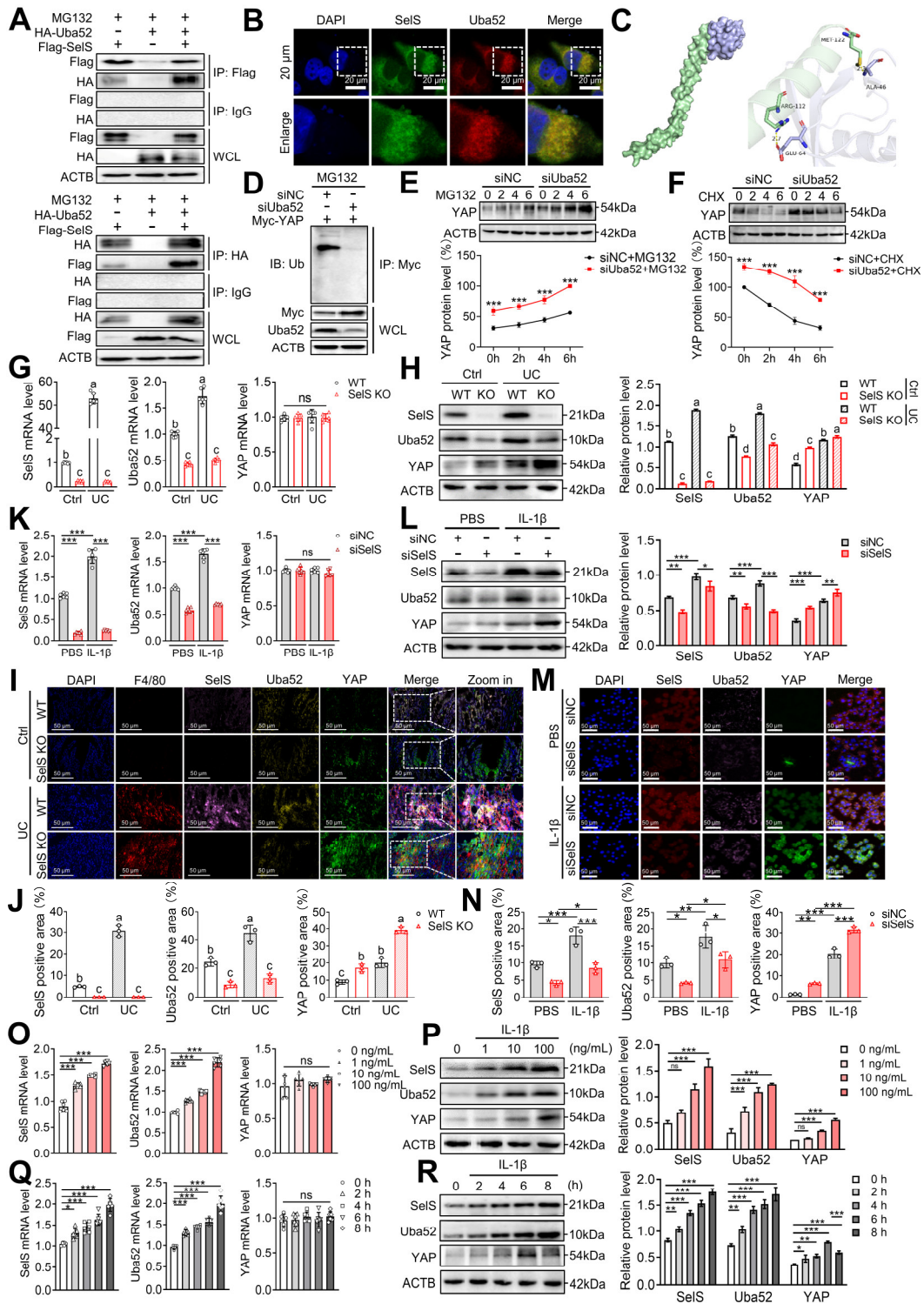
Figure 3. SelS negatively regulates the stability of macrophage YAP by promoting the Uba52-dependent proteasome degradation pathway. (A) The IB of Flag or HA was followed by immunoprecipitation (IP) with anti-HA antibody or anti-Flag antibody in whole-cell lysates (WCL) of J774.1, n = 3. **(B)** Immunofluorescence co-localization of SelS and Uba52 in J774.1, n = 3. Scale

bar, 20 μm. **(C)** Molecular docking pattern diagram of SelS and Uba52. **(D)** J774.1 were

cotransfected with Myc-YAP in the presence or absence of siUba52 and then treated with MG132

(10 mM) for 6 h. The cell lysates were subjected to IP with anti-Myc beads and immunoblotted with

the ubiquitination antibody, n = 3. **(E)** J774.1 were pretreated with siNC or siUba52 and then

incubated with MG132 (10 mM) for indicated time points. WB analysis of endogenous YAP, n = 3.

(F) J774.1 were pretreated with siNC or siUba52. Subsequently, stimulated with IL-1β for 6 h before

being incubated with CHX (50 mg/mL) for indicated time points. WB analysis of endogenous YAP,

n = 3. **(G-J)** WT and SelS KO mice were treated with or without 3.5% DSS for 7 d. **(G-H)** mRNA

(n = 6) and protein (n = 3) expression of SelS, Uba52 and YAP in the colon. Different lowercase

letters indicate significant differences between groups. **(I-J)** Immunofluorescence staining and

quantitative analysis of SelS, Uba52, and YAP in the colon. n = 3. Scale bar, 50 μm. Different

lowercase letters indicate significant differences between groups. **(K-N)** J774.1 transfected with

siNC or siSelS were treated with PBS or IL-1β (100 ng/mL) for 6 h. **(K-L)** mRNA (n = 6) and

protein (n = 3) expression of SelS, Uba52, and YAP in J774.1. **(M-N)** Immunofluorescence staining

and quantitative analysis of SelS, Uba52, and YAP in J774.1. n = 3. Scale bar, 50 μm. **(O-P)** J774.1

were stimulated with indicated concentrations of IL-1β for 6 h. mRNA (n = 6) and protein (n = 3)

expression of SelS, Uba52, and YAP. **(Q-R)** J774.1 were treated with IL-1β (100 ng/mL) for the

indicated times. mRNA (n = 6) and protein (n = 3) expression of SelS, Uba52, and YAP.
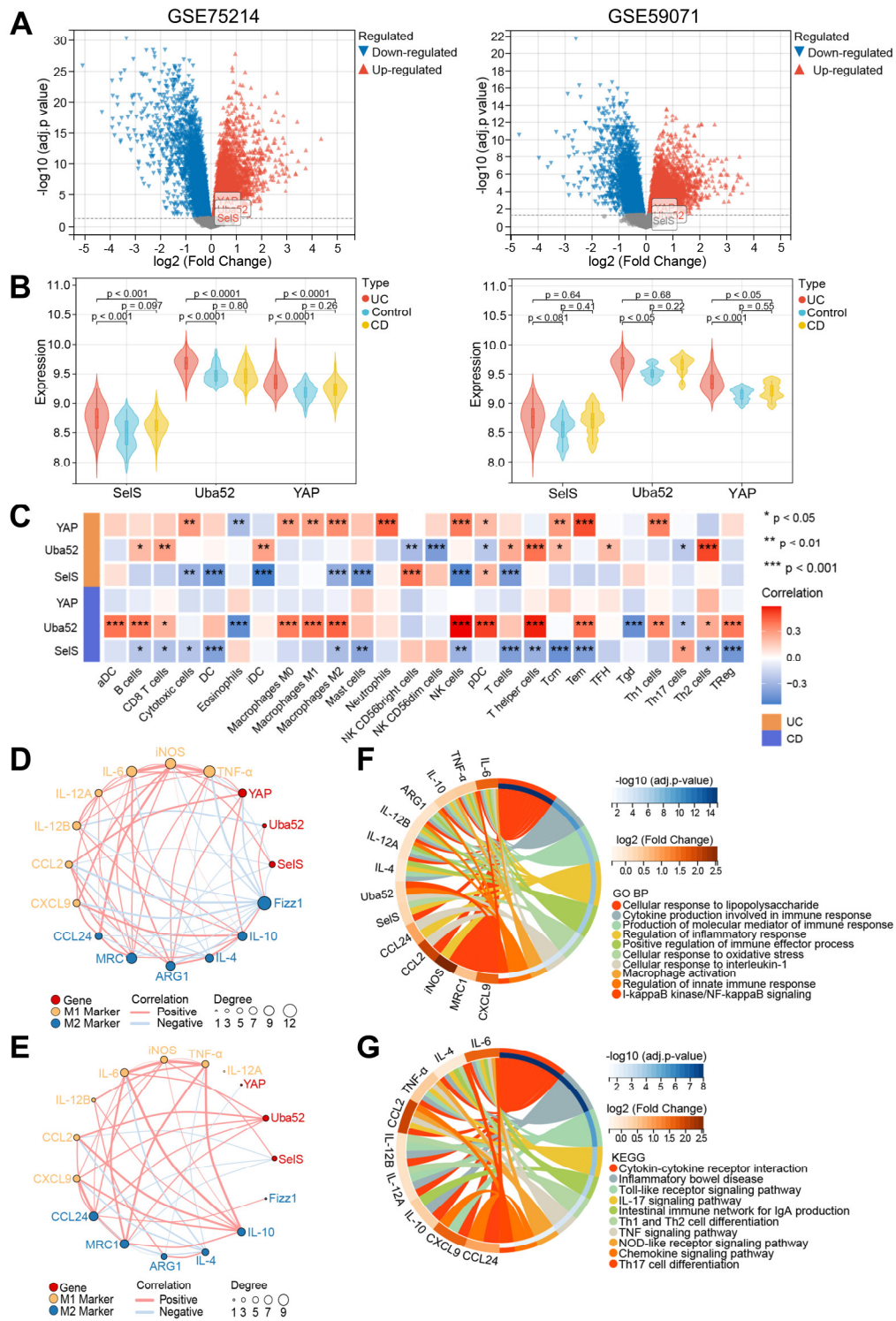
Figure 4. Relationship between SelS, Uba52, and YAP and macrophage polarization in the colon of IBD patients mined by GEO data. (A) Volcano plot depicting DEGs between healthy individuals and IBD patients in the GSE75214 and GSE59071 datasets. **(B)** Violin plots depicting differences in SelS, Uba52, and YAP expression between healthy individuals and IBD patients in

896   the GSE75214 and GSE59071 datasets. **(C)** Heatmap indicates the correlation of SelS, Uba52, and

897   YAP with 26 immune cell subpopulations in the TCGA dataset. **(D)** Correlation between SelS,

898   Uba52, YAP, and M1/M2 macrophage polarization markers in UC patients in the GSE75214 dataset.

899   **(E)** Correlation between SelS, Uba52, YAP, and M1/M2 macrophage polarization markers in CD

900   patients in the GSE75214 dataset. **(F)** Biological processes (BP) analyzed by GO functional

901   annotation of gene sets consisting of SelS, Uba52, YAP, and M1/M2 biomarkers. **(G)** KEGG

902   enrichment analysis of gene sets composed of SelS, Uba52, YAP, and M1/M2 biomarkers.
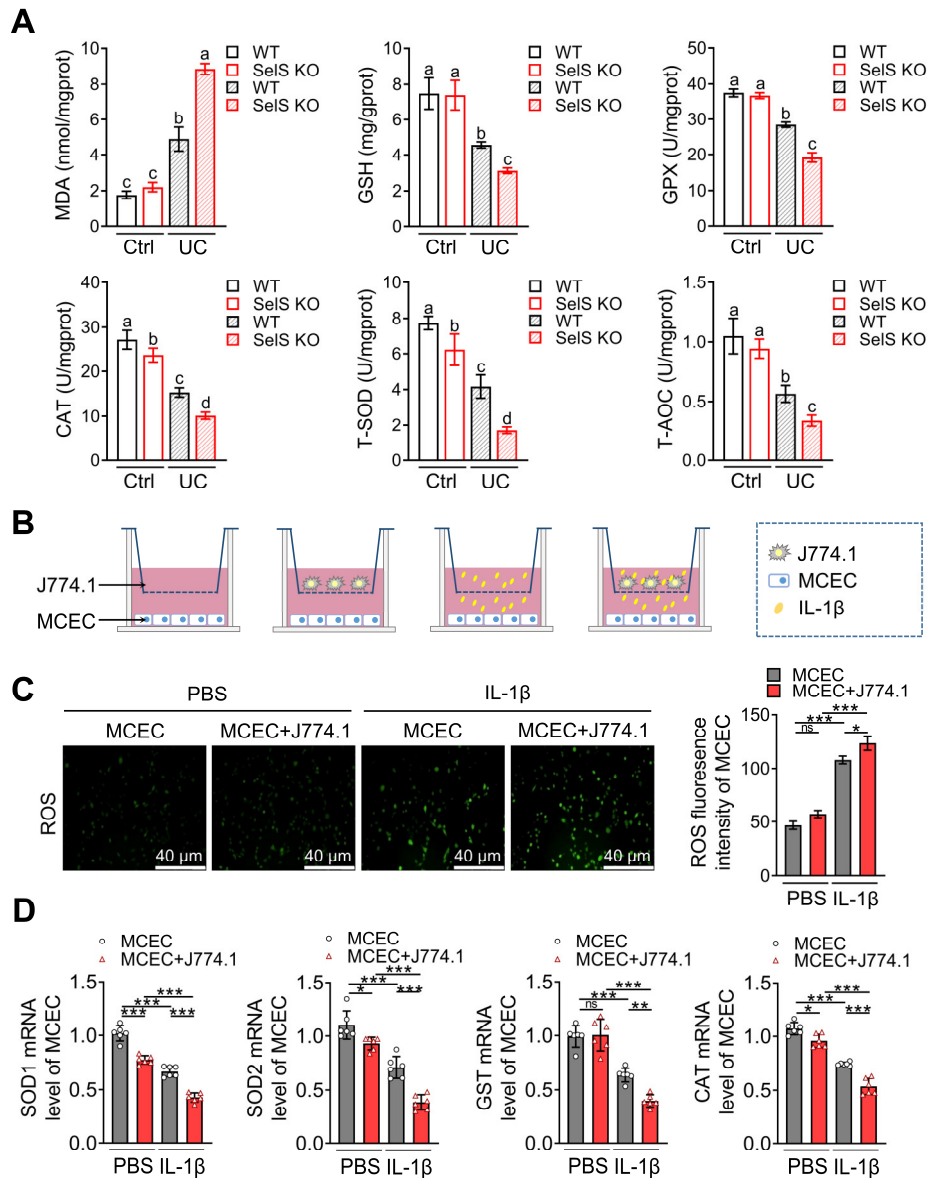
Figure 5. SelS deletion exacerbates oxidative stress in the colon of UC mice involves M1 macrophages inducing ROS overproduction in CECs. (A) Levels of pro-oxidant indicators (MDA) and antioxidant markers (GSH, GPX, CAT, T-SOD, and T-AOC) in the colon of WT and SelS KO mice in Ctrl and UC groups, n = 6. Different lowercase letters indicate significant differences between groups. **(B-D)** MCECs were cocultured with J774.1 under IL-1β (100 ng/mL) stimulation. **(B)** Coculture pattern diagram of MCECs and J774.1. **(C)** Representative images and quantitative analysis of ROS levels in MCECs, n = 3. Scale bar, 40 μm. **(D)** mRNA expression of antioxidase in MCECs, n = 6.

912
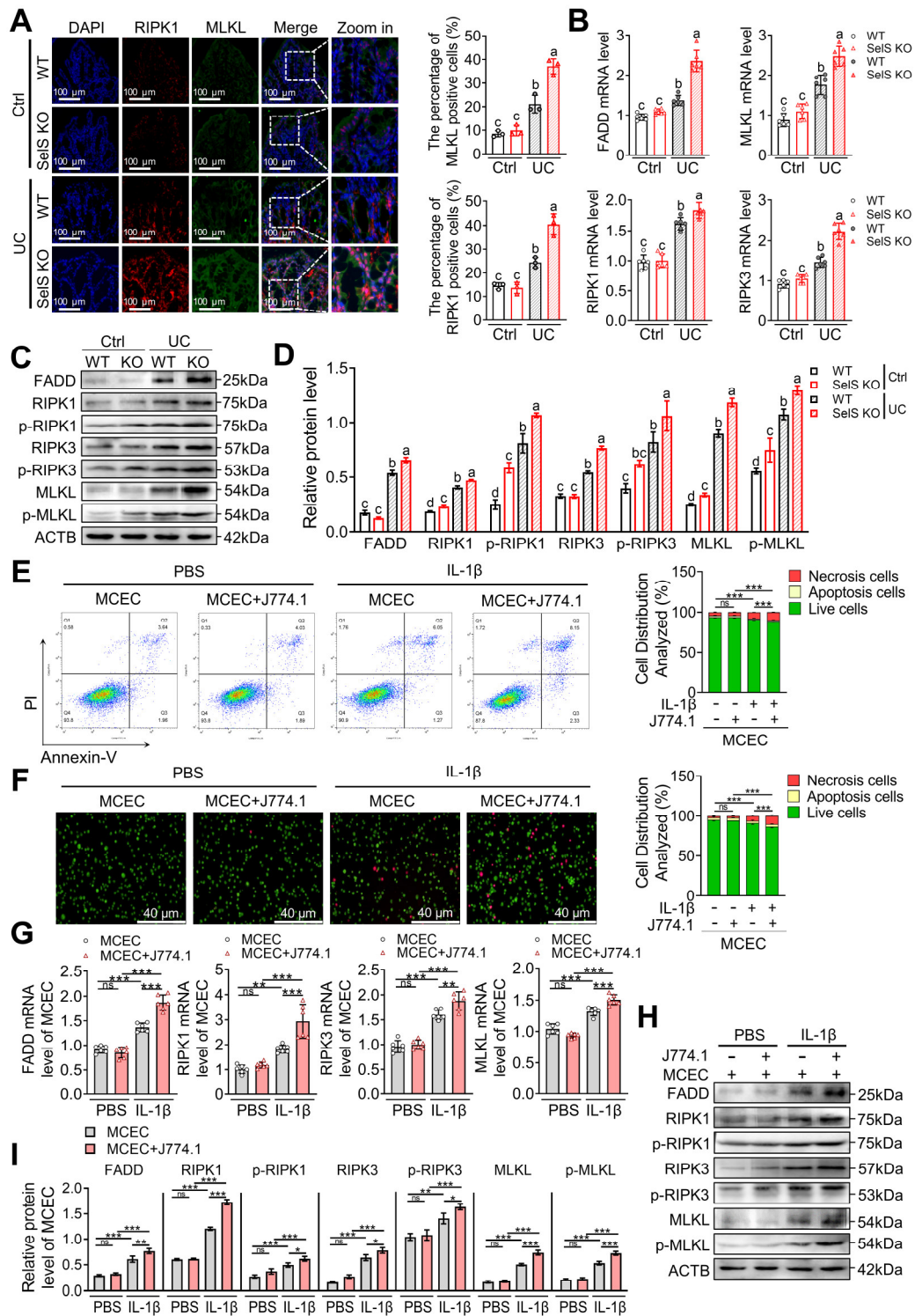
Figure 6. SelS deletion promotes necroptosis in the colon of UC mice involves M1 macrophages

inducing oxidative stress in CECs. (A) Immunofluorescence staining and quantitative analysis of

RIPK1 and MLKL in the colon of WT and SelS KO mice in Ctrl and UC groups, n = 3. Scale bar,

100 μm. Different lowercase letters indicate significant differences between groups. **(B)** mRNA

917   expressions related to necroptosis in the colon of WT and SelS KO mice in Ctrl and UC groups, n

918   = 6. Different lowercase letters indicate significant differences between groups. **(C-D)** Protein levels

919   related to necroptosis in the colon of WT and SelS KO mice in Ctrl and UC groups, n = 3. Different

920   lowercase letters indicate significant differences between groups. **(E-I)** MCECs were cocultured

921   with J774.1 under IL-1β (100 ng/mL) stimulation. **(E)** Flow cytometry detection and quantification

922   analysis for FITC/PI staining in MCECs, n = 3. **(F)** AO/EB staining and quantitative analysis in

923   MCECs, n = 3. Scale bar, 40 μm. **(G)** mRNA expressions related to necroptosis in MCECs, n = 6.

924   **(H-I)** Protein levels related to necroptosis in MCECs, n = 3.

925
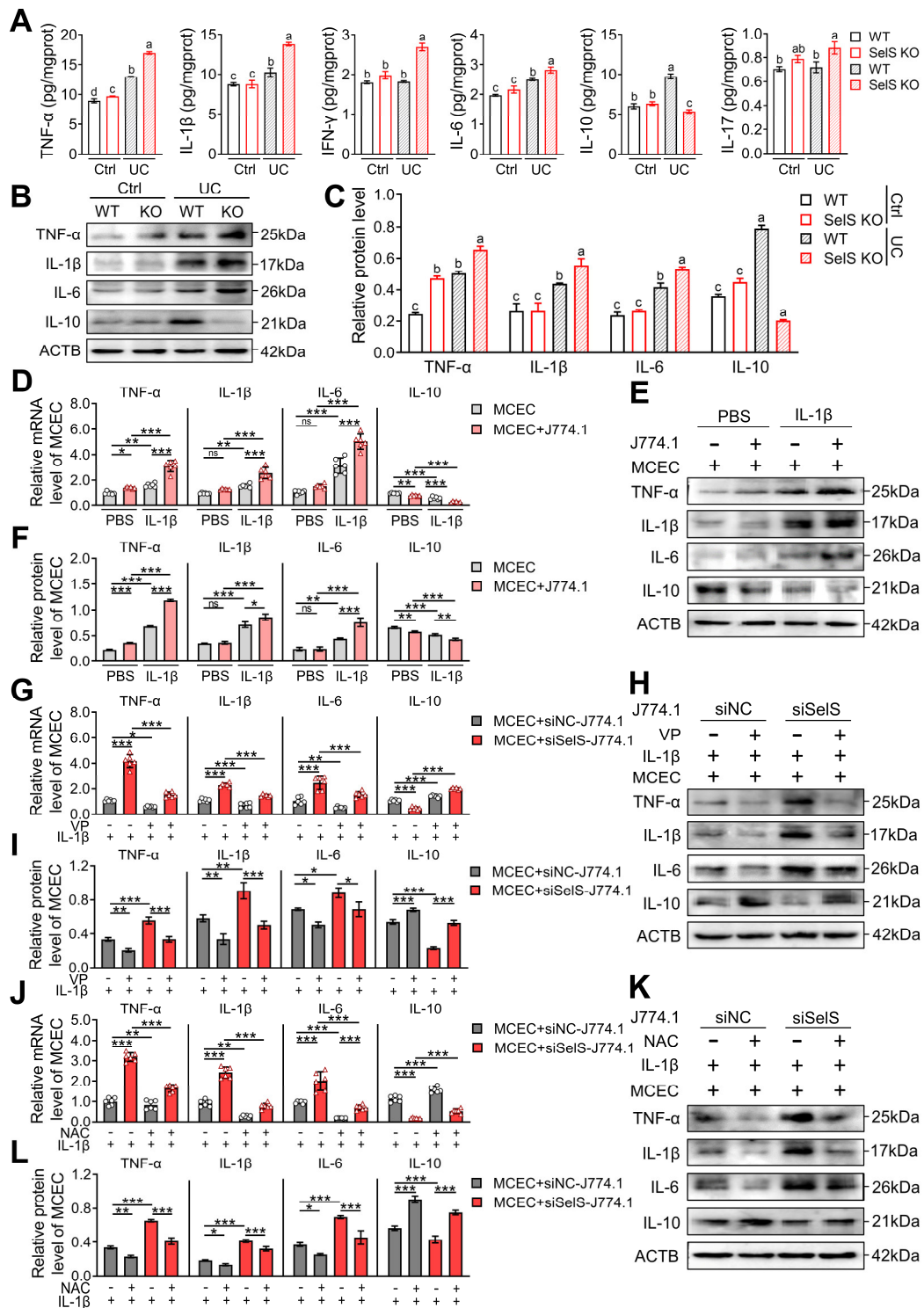
Figure 7. SelS deletion amplifies inflammatory response relies on M1 polarization-induced

oxidative stress in CECs. (A) Inflammatory cytokine levels in the colon of WT and SelS KO mice

in Ctrl and UC groups, n = 6. Different lowercase letters indicate significant differences between

groups. **(B-C)** Protein levels related to inflammatory cytokine in the colon of WT and SelS KO mice

930 in Ctrl and UC groups, n = 3. Different lowercase letters indicate significant differences between

931 groups. **(D-F)** MCECs were cocultured with J774.1 under IL-1β (100 ng/mL) stimulation. **(D)**

932 mRNA expressions related to inflammatory cytokine in MCECs, n = 6. **(E-F)** Protein levels related

933 to inflammatory cytokine in MCEC, n = 3. **(G-I)** MCECs were cocultured with VP (0.32 μM)-

934 pretreated siNC or siSelS J774.1 under IL-1β (100 ng/mL) stimulation. **(G)** mRNA expressions

935 related to inflammatory cytokine in MCECs, n = 6. **(H-I)** Protein levels related to inflammatory

936 cytokine in MCECs, n = 3. **(J-L)** 1 mM NAC-pretreated MCECs were cocultured with siNC or

937 siSelS J774.1 under IL-1β (100 ng/mL) stimulation. **(J)** mRNA expressions related to inflammatory

938 cytokine in MCECs, n = 6. **(K-L)** Protein levels related to inflammatory cytokine in MCECs, n = 3.
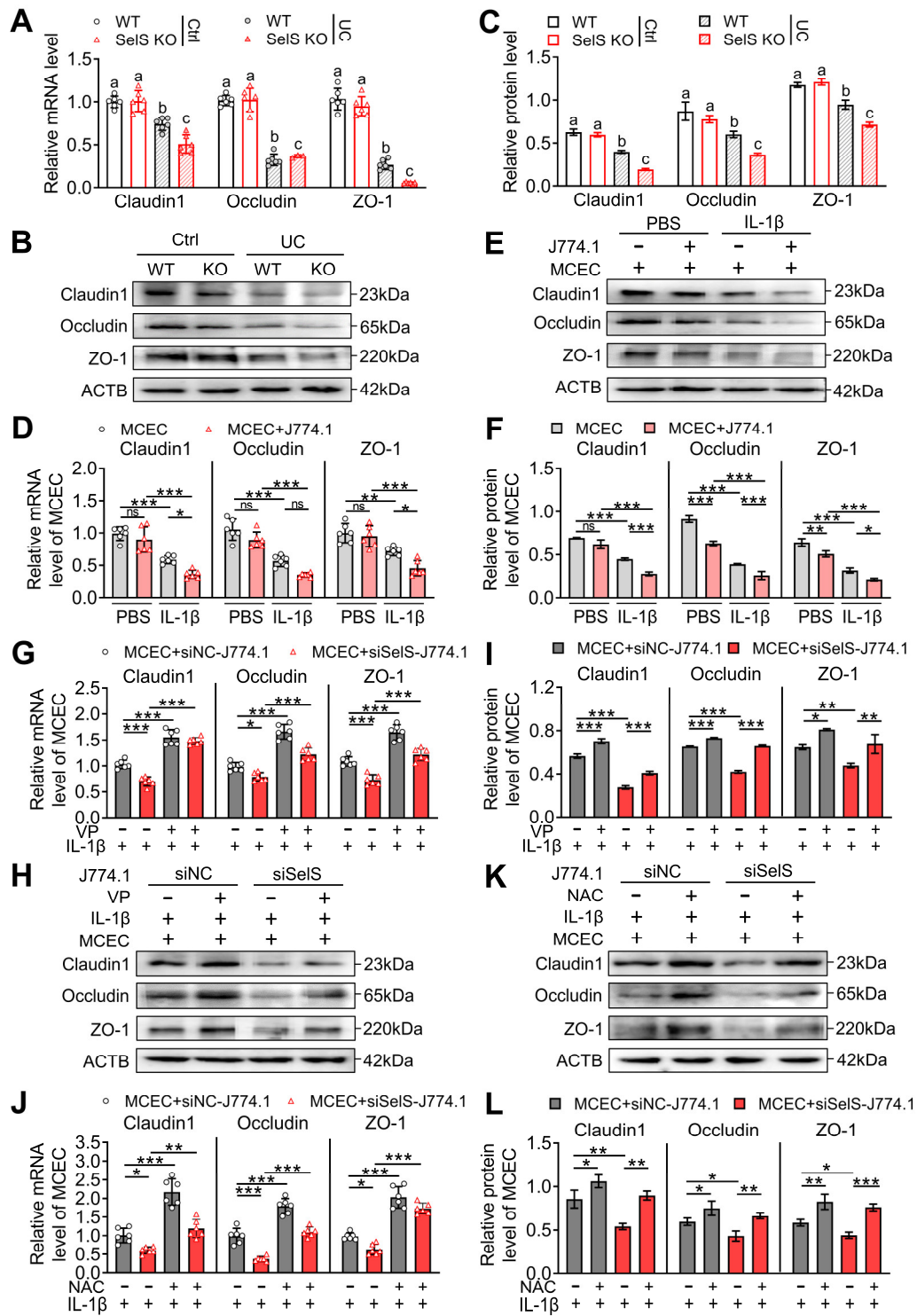
Figure 8. SelS deletion aggravates tight junction dysfunction dependent on M1 polarization-induced oxidative stress in CECs. (A) mRNA expressions related to tight junction in the colon of WT and SelS KO mice in Ctrl and UC groups, n = 6. Different lowercase letters indicate significant differences between groups. **(B-C)** Protein levels related to tight junction in the colon of WT and

944   SelS KO mice in Ctrl and UC groups, n = 3. Different lowercase letters indicate significant

945   differences between groups. **(D-F)** MCECs were cocultured with J774.1 under IL-1β (100 ng/mL)

946   stimulation. **(D)** mRNA expressions related to tight junction in MCECs, n = 6. **(E-F)** Protein levels

947   related to tight junction in MCECs, n = 3. **(G-I)** MCECs were cocultured with VP (0.32 μM)-

948   pretreated siNC or siSelS J774.1 under IL-1β (100 ng/mL) stimulation. **(G)** mRNA expressions

949   related to tight junction in MCECs, n = 6. **(H-I)** Protein levels related to tight junction in MCECs,

950   n = 3. **(J-L)** 1 mM NAC-pretreated MCECs were cocultured with siNC or siSelS J774.1 under IL-

951   1β (100 ng/mL) stimulation. **(J)** mRNA expressions related to tight junction in MCECs, n = 6. **(K-**

952   **L)** Protein levels related to tight junction in MCECs, n = 3.

953
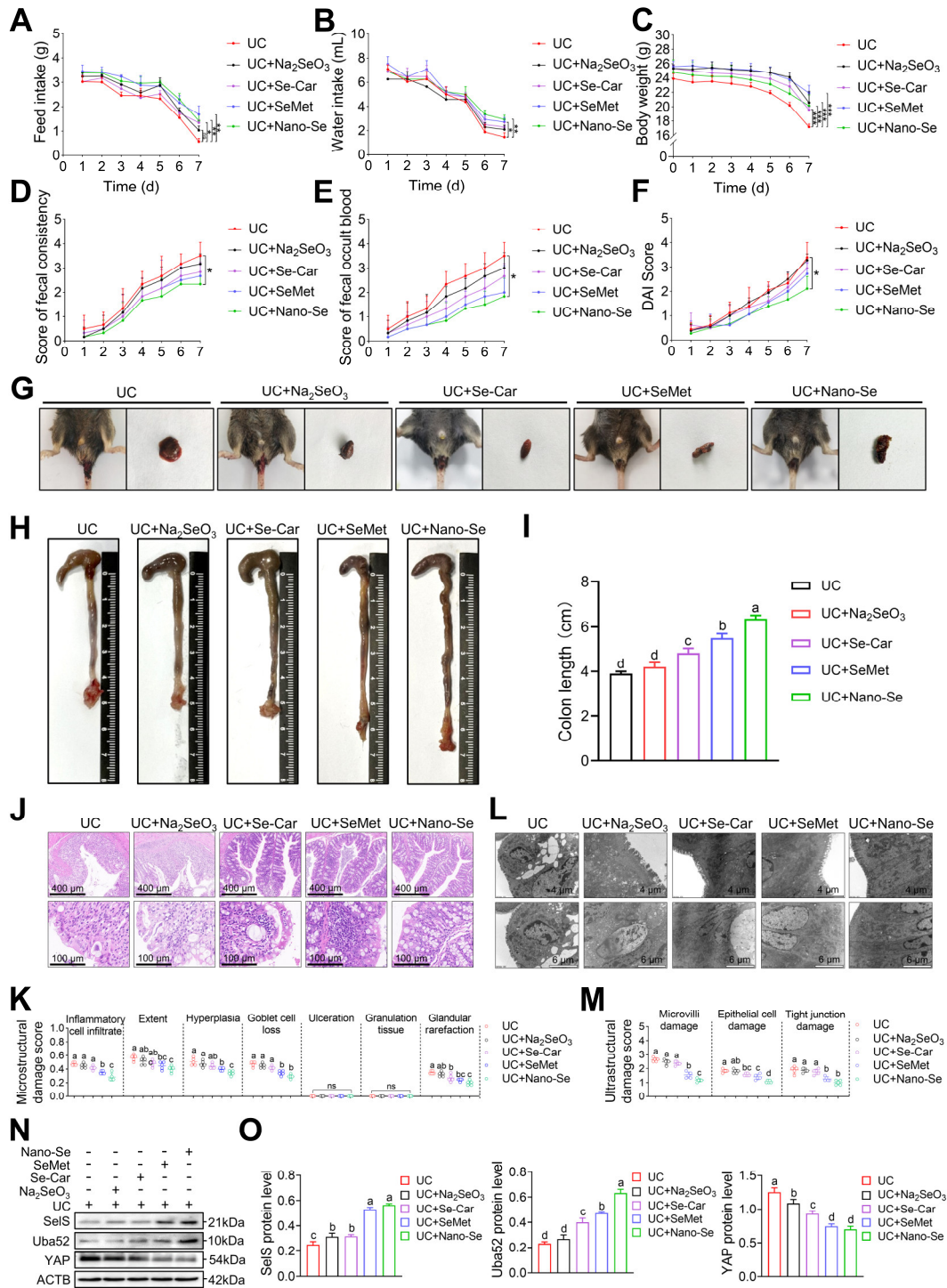
Figure 9. Selenium supplementation attenuates colon injury in UC mice. (A-F) Clinical

indicators of WT mice with UC given selenium supplements containing 2 mg/kg selenium, n = 6.

(A) Feed intake. **(B)** Water intake. **(C)** Body weight. **(D)** Scores of fecal consistency. **(E)** Scores of

fecal occult blood. **(F)** DAI score. **(G)** Perianal area and feces appearance of UC mice. **(H-I)** Colon

958   length, n = 6. Different lowercase letters indicate significant differences between groups. **(J)**

959   Representative H&E slides of distal colon sections, n = 6. Scale bar, 400 μm and 100 μm. **(K)** The

960   microstructural damage score of colon tissue, n = 6. Different lowercase letters indicate significant

961   differences between groups. **(L)** Representative images of TEM detection for the colon tissue, n =

962   6. Scale bar, 4 μm and 6 μm. **(M)** The ultrastructural damage score of the colon tissue, n = 6.

963   Different lowercase letters indicate significant differences between groups. **(N-O)** Protein levels of

964   SelS, Uba52, and YAP in the colon, n = 3. Different lowercase letters indicate significant differences

965   between groups.